AD

(12)

TECHNICAL REPORT BRL-TR-2808

FIN GAPS AND BODY SLOTS OF GUIDED PROJECTILES: EFFECTS, DATA CORRELATION AND MODELING

AMEER G. MIKHAIL

JUNE 1987

US ARMY BALLISTIC RESEARCH LABORATORY
ABERDEEN PROVING GROUND, MARYLAND

UNCLASSIFIED
SECURITY CLASSIFICATION OF THIS PAGE

A184445

REPORT DOCUMENTATION PAGE

Form Approved
OMB No 0704-0188
Exp. Date Jun 30, 1986

1a. REPORT SECURITY CLASSIFICATION: UNCLASSIFIED	1b. RESTRICTIVE MARKINGS
2a. SECURITY CLASSIFICATION AUTHORITY	3. DISTRIBUTION/AVAILABILITY OF REPORT: Approved for public release, distribution unlimited.
2b. DECLASSIFICATION/DOWNGRADING SCHEDULE	
4. PERFORMING ORGANIZATION REPORT NUMBER(S)	5. MONITORING ORGANIZATION REPORT NUMBER(S)
6a. NAME OF PERFORMING ORGANIZATION: U.S. Army Ballistic Research Laboratory; 6b. OFFICE SYMBOL (If applicable): SLCBR-LF	7a. NAME OF MONITORING ORGANIZATION
6c. ADDRESS (City, State, and ZIP Code): Aberdeen Proving Ground, MD 21005-5066	7b. ADDRESS (City, State, and ZIP Code)
8a. NAME OF FUNDING/SPONSORING ORGANIZATION; 8b. OFFICE SYMBOL (If applicable)	9. PROCUREMENT INSTRUMENT IDENTIFICATION NUMBER
8c. ADDRESS (City, State, and ZIP Code)	10. SOURCE OF FUNDING NUMBERS

PROGRAM ELEMENT NO.	PROJECT NO.	TASK NO.	WORK UNIT ACCESSION NO
62618A	1L162618AH80	00	001 AJ

11. TITLE (Include Security Classification)

FIN GAPS AND BODY SLOTS OF GUIDED PROJECTILES: EFFECTS, DATA CORRELATION AND MODELING

12. PERSONAL AUTHOR(S)
MIKHAIL, AMEER G.

13a. TYPE OF REPORT	13b. TIME COVERED	14. DATE OF REPORT (Year, Month, Day)	15. PAGE COUNT
Tehnical Report	FROM _____ TO _____		

16. SUPPLEMENTARY NOTATION

17. COSATI CODES			18. SUBJECT TERMS (Continue on reverse if necessary and identify by block number)
FIELD	GROUP	SUB-GROUP	Guided Projectiles; Fin-Body Gap Effect; Aerodynamic Prediction; Body-Slot Effect; Fast Aerodynamic Codes; The Copperhead Projectile
01	01		
19	01		

19. ABSTRACT (Continue on reverse if necessary and identify by block number)

All prior work concerned with the effect of streamwise fin-body gaps (unporting effect and body slots on the fin loads of missiles and projectiles in the transonic speed regime of $0.8 < M < 1.2$, has been surveyed and analyzed. All known experimental data for the gap effects have been analyzed. A correlation relation was established to predict fin normal force losses due to gaps for any fin shape, size, aspect ratio, gap to body diameter ratio, body diameter and flow Reynolds number. The results agree very well with the data which span a large variation in Reynolds number, body diameter and boundary layer thickness. Although the Mach range for present model was intended to be $0.8 < M < 1.2$, available data indicated its validity in the wider range of $0.7 < M < 1.6$. Fifteen cases were utilized to validate the present gap model. The slot effect model utilized is that of Washington et al. Application of these two

20 DISTRIBUTION/AVAILABILITY OF ABSTRACT	21 ABSTRACT SECURITY CLASSIFICATION
☒ UNCLASSIFIED/UNLIMITED ☐ SAME AS RPT. ☐ DTIC USERS	UNCLASSIFIED

22a NAME OF RESPONSIBLE INDIVIDUAL	22b TELEPHONE (Include Area Code)	22c OFFICE SYMBOL
Ameer G. Mikhail	(301) 278-3773	SLCBR-LF-R

DD FORM 1473, 84 MAR — 83 APR edition may be used until exhausted. All other editions are obsolete

SECURITY CLASSIFICATION OF THIS PAGE

UNCLASSIFIED

19. ABSTRACT (Continued)

corrections to the Copperhead guided projectile was made and a reduction as large as 38% was predicted for the normal force, which was then validated by the experimental data. The present results can be used for estimating fin load losses for the fin design of guided projectiles and missiles, with accuracy of 5%, over the intended Mach number range $0.8 \leq M \leq 1.2$.

TABLE OF CONTENTS

Page

LIST OF FIGURES..... v

I. INTRODUCTION..... 1

1. GAP EFFECTS..... 1
2. SLOT EFFECTS..... 2

II. ANALYSIS..... 2

1. GAP EFFECTS..... 2
   a. Details of the experimental data and test conditions..... 2
   b. The correlation relation..... 2
2. SLOT EFFECTS..... 8

III. RESULTS..... 8

1. GAP EFFECTS..... 8
   a. Validation of the gap model..... 8
   b. Application to the Copperhead projectile..... 9
2. SLOT EFFECTS: APPLICATION TO THE COPPERHEAD PROJECTILE.....10
3. COMBINED GAP AND SLOT EFFECTS.....10

IV. CONCLUSIONS.....11

REFERENCES.....37

LIST OF SYMBOLS.....39

DISTRIBUTION LIST.....41

LIST OF FIGURES

Figure		Page
1	Configuration of the Copperhead projectile	12
2	Copperhead tail fin and gap configuration	13
3	Wind tunnel model configurations	14
4	Wind tunnel model configurations	15
5	Details of fin panel configurations	16
6	Details of fin panel configurations	17
7	Test conditions for all known data utilized	18
8	Nomenclature for the correlation analysis	19
9	Examples of fin area desgination for several fin planforms	20
10	Transonic wind tunnel data for triangular fin of AR = 1.5	21
11	Wind tunnel data for rectangular fin of AR = 1.0	22
12	Case designation for fifteen correlation tests used for validation	23
13a	Comparison with data of Killough, rectangular fin of AR = 1.0	24
13b	Comparison with data of Killough, rectangular fin of AR = 3.0	25
14a	Comparison with data of Dahlke and Pettis, rectangular fin of AR = 1.0	26
14b	Comparison with data of Dahlke and Pettis, rectangular fin of AR = 0.5	27
15	Comparison with data of Henderson, rectangular fin of AR = 1.671	28
16	Comparison with data of Fellows, rectangular fin of AR = 2.22	29
17	Gap modeling effect on the normal force slope coefficient for the Copperhead projectile	30
18	Gap modeling effect on the pitching moment slope coefficient for the Copperhead projectile	31
19	Slot configurations for the Copperhead projectile (from Reference 12)	32

LIST OF FIGURES (Continued)

Figure		Page
20	Slot modeling effect on the normal force slope coefficient for the Copperhead projectile	33
21	Slot modeling effect on the pitching moment slope coefficient for the Copperhead projectile	34
22	Gap and slot modeling effects on the normal force slope coefficient for the Copperhead projectile	35
23	Gap and slot modeling effects on the pitching moment slope coefficient for the Copperhead projectile	36

I. INTRODUCTION

As reported in Reference 1, large deviations were found between both the pitching moment and normal force predictions and the wind tunnel data for the aerodynamic prediction of the Copperhead guided projectile, shown in Figure 1. Two predictions were made using the fast aerodynamic design codes of the Missile DATCOM and the NSWCAP, both of which are described in Reference 1. This deviation was as large as 38% at $M \approx 1$ and was still quite large in the transonic speed regime of $0.8 < M < 1.2$. This deviation was significantly smaller outside that speed regime, in the wider regime between $0.5 \leq M \leq 1.8$. This large deviation was attributed mainly to the effects of the tail fin gaps and the open slots in the projectile body. These slots are used to house the fin blades before in-flight deployment. The tail fin geometry and the associated streamwise gaps are shown in Figure 2 .

It is the purpose of this paper to correct for the normal force losses of the fins due to streamwise fin-body gaps and body slots, in the transonic regime $0.8 \leq M \leq 1.2$. All existing data concerned with these effects has been surveyed and utilized for establishing the present correlations.

1. GAP EFFECTS

It seems that Bleviss and Struble[2] in 1953 were first to present an inviscid analysis of gap losses for triangular fins at supersonic speeds, $M > 1$. The analysis is only valid for triangular fins and is not applicable for small gap to diameter ratios, where viscosity effects are dominant. The analysis also assumes a long afterbody extending beyond the fin location. Streamwise gap refers to the gap existing when the control surface is aligned along the axial direction of the body. Almost at the same time, Mirles[3] presented a slender body analytic solution for the fin lift losses, with the same triangular fin and long afterbody limitations. Therefore, his results, not surprisingly, were close to those of Reference 2. Shortly after, in 1954, Dugan and Hikido[4] also presented a slender body analysis for gap effects for triangular fins mounted on long after bodies. The results, being based on slender body theory, are Mach number independent. Also they are not restricted to supersonic speeds only. Hoerner,[5] in a book published in 1975, refers to some very early experiment (probably in the 1940's) at very low subsonic speeds for low fin aspect ratios. The presented data is very sparse and the test conditions are very ambiguous.

In 1964, the first wind tunnel tests for gap effects were presented by Killough.[6] Data was provided for three rectangular fins of aspect ratios of 1.0, 2.0 and 3.0; in the Mach range of 0.8 to 4.5 . Similar wind tunnel data were obtained later by Dahlke and Pettis[7] in 1970 for a single triangular fin of AR = 1.5 and three rectangular fins of AR = 0.5, .75 and 1.0 . These fins were tested in the Mach range of 0.8 to 4.0, for four gap heights. In 1977, although studying other effects, Henderson[8] tested a rectangular fin of AR = 1.67 for a single gap height in the Mach range $0.8 \leq M \leq 1.2$. Fellows,[9] in 1982, provided subsonic data for two sets of rectangular fins of AR = 1.67 and 2.22 for very small gap heights.

August,[10] in 1982, used the inviscid supersonic analysis of Bleviss and Struble and the manipulated results of Hoerner at subsonic speeds, to estimate the normal force losses for streamwise gaps. The application was made to the

typical triangular fin of aspect ratio 1.0 . August applied the analysis to the Sidewinder missile geometry at M = 2.5 for the triangular canard fin with fin deflection. The gap area was estimated and equalized by a streamwise gap area. This application was done during the development of a fast aerodynamic design code. Sun et al,[11] in 1984, re-iterated the results of August and made an application to a missile configuration at M = 1.2 and 2.0 using the same computer code.

2. SLOT EFFECTS

Less exhaustive data or analyses have been pursued for the slot effects than those pursued for the gap effects. In 1979, Appich and Wittmeyer[12] tested a full scale model of the Copperhead projectile and reported the effect of closing the slots on the normal force and drag of the projectile in the Mach range of 0.5 to 1.8 . However, results were presented only for M = 0.5 and 1.5 . Washington et al[13] analyzed the data of Appich[12] and suggested a simple model to correct for the normal force losses due to the slots. This correction utilizes the slender body theory and therefore is independent of the Mach number. However, applications were only made to subsonic speeds of 0.5, .8 and .95 . The same results were summarized later in Reference 14. The axial force and drag contribution of the slots were studied and reported separately by Appich et al in 1980.[15]

II. ANALYSIS

1. GAP EFFECTS

An analytic correlation for the fin-body gap effects was established, taking into account all existing data for fin gaps. This correlation is intended for the transonic Mach range of $0.8 \leq M \leq 1.2$. However, existing data showed its applicability in the wider range of $0.7 < M < 1.8$ without any loss in accuracy.

a. Details of the experimental data and test conditions The four wind tunnel data sets of References (6-9) were used. The exact body configuration for each test is given in Figures 3 and 4. The corresponding fin shape and dimensions are given in detail in Figures 5 and 6. The test conditions, including Mach and Reynolds numbers, gap height, gap area to fin area ratio, for each case are given in Figure 7.

b. The correlation relation Based on the familiar work of Pitts, Nielsen and Kattari,[16] the normal force coefficient of a combined missile body and fins is usually written as

$$C_{N_{BT}} = C_{N_B} + (K_{T(B)} + K_{B(T)})C_{N_T} \qquad (1)$$

where: the subscripts B, T and BT stand for body alone, tail alone and body-tail combination, respectively;

$K_{T(B)}$ is the interference factor representing the increase of tail fin lift due to the existence of a nearby body, and is usually referred to as the "body up-wash" effect; and

$K_{B(T)}$ is the interference factor representing the increase of body lift due to the existence of a near-by tail fin, and is usually referred to as the "carry-over factor." It is represented as a small fraction of the fin-alone lift.

In the present work "C_{N_f}" will be used to denote the fin normal force plus the two mentioned interference effects, i.e. Equation (1) can be written as

$$C_{N_{BT}} = C_{N_B} + C_{N_f} \tag{2}$$

For a gap of any size, the lift (and therefore the normal force) produced by a fin would always be less than that produced without a gap. Therefore a normal force loss factor, FNF, is introduced and is defined as

$$FNF = \frac{C_{N_{fg}}}{C_{N_f}} = \frac{C_{N_{\alpha fg}}}{C_{N_{\alpha f}}} \tag{3}$$

where $C_{N_{fg}}$ is the normal force of the fin (including interference effects) in the presence of a gap. The second equality sign in Equation 3 is valid only for small angles of attack, usually less than $\pm 6°$. For a case with gap, one could easily model the effect of a gap if the loss factor FNF was known. This modeling is achieved through the equation

$$C_{N_{BT}} = C_{N_B} + FNF \cdot (K_{T(B)} + K_{B(T)})C_{N_T} \tag{4}$$

One approach considered for modeling was to correct the analysis of Bleviss and Struble of triangular fins to account for viscosity and the shape of fin planform. The baseline case would be the triangular fin data of Dahlke and Pettis. However, this approach was not chosen in favor of a different approach. The new approach is to make all corrections and/or correlations based on the same triangular fin shape for which an inviscid analysis is valid, and to base all the correlation relations on experimental data. Therefore, the FNF factor was computed for all the test cases of References 6-9 and their wind tunnel test conditions were determined. The intent was to correlate a known FNF for a known fin planform of certain gap height mounted on a particular body diameter in a flow of particular Reynolds number, to the FNF of a totally different fin with all different parameters. Figure 8 shows fin configurations 1 and 2 where subscript 1 will always refer to the known case

and 2 to the unknown case. The planform of fin 2 is split into two parts: a basic triangular configuration of area A_{22} and second part is the remainder of the planform area, with area of A_{20}. Examples of the area A_{22} designation for several fin planforms are given in Figure 9.

The FNF factor is thought to be function of several parameters:

FNF = FNF (fin area, fin shape, fin gap height, gap to diameter ratio, Reynolds number at the leading edge of fin, fin aspect ratio, Mach number).

The last two parameters were later deleted due to the following reasons. The aspect ratio was substituted by boch the fin area and fin shape parameters. The fin shape not only is represented by a description factor (e.g., triangular or rectangular) but also by the root chord and the semi span height. The Mach number dependency in the FNF function was dropped when the data of Dahlke et al was analyzed in the transonic region of $0.8 \leq M \leq 1.2$. This data, an example of which is given in Figure 10, showed no variation of the FNF with Mach number. This behavior was noticed in all data. Thus, although both C_{N_f} and $C_{N_{fg}}$ do change, their ratio is always constant in that transonic speed range. Furthermore, by computing the FNF factor for another fin planform of Dahlke et al, one can note, that the Mach number independence extends further between $M = .7$ and 1.8 . This observation is depicted in Figure 11. One also can note the surprising change in FNF in the subsonic region $M < 0.7$. For that reason, i.e. the rapid change in FNF in the subsonic region, the results of Hoerner should be used with caution.

The basic correlation formula relates the unknown case 2 to the known case 1 through the overall correlation factor, CF, as:

$$\left.\frac{C_{N_{\alpha fg}}}{C_{N_{\alpha f}}}\right|_2 = CF \cdot \left.\frac{C_{N_{\alpha fg}}}{C_{N_{\alpha f}}}\right|_1 , \qquad (5)$$

i.e.,

$$FNF_2 = CF \cdot FNF_1$$

This overall correlation factor itself is split into a multiple of several factors. They are: the fin shape factor, SF; the fin area factor, AF; the fin gap factor, GF; the fin chord/span factor, CSF; and the boundary layer factor, BF. Therefore one can write:

$$\left.\frac{C_{N_{\alpha fg}}}{C_{N_{\alpha f}}}\right|_2 \equiv FNF_2 = CF \cdot FNF_1$$

$$= [SF \cdot AF \cdot GF \cdot CSF \cdot BF] \cdot \left.\frac{C_{N_{\alpha fg}}}{C_{N_{\alpha f}}}\right|_1 \qquad (6)$$

i) The shape factor, SF, was originally formulated as:

$$SF = \left(\frac{A_2}{A_{22}}\right) \Big/ \left(\frac{A_1}{A_{11}}\right) = \left(\frac{A_{22} + A_{20}}{A_{22}}\right) \Big/ \left(\frac{A_{11} + A_{10}}{A_{11}}\right). \qquad (7)$$

This gives a value of:

2 for general correlation from a triangular to a rectangular fin shape and

1 for general correlation from a rectangular to recangular fin.

However, from the data of Dahlke et al, it was found that SF should be 1.76 for a triangular to rectangular shape correlation with $A_{22} = A_{11}$ and with all other conditions fixed. This was finally achieved by modeling relation (7) into a slightly more complex form.

$$SF = \frac{\left[\left(\frac{.76A_{20}+A_{22}}{A_{22}}\right) + \left(\frac{.24A_{20}(A_{22}-A_{11})}{(.5b_2c_2)(.5b_2c_2-.5b_1c_1)}\right)\right]}{\left[\left(\frac{(.76A_{10}+A_{11})}{A_{11}}\right) + \left(\frac{.24A_{10}(A_{22}-A_{11})}{(.5b_1c_1)(.5b_2c_2-.5b_1c_1)}\right)\right]} \qquad (8a)$$

One can therefore easily track the origin for the split-up factors of .76 and .24. Also one can note that the second term in each bracket will drop out if $A_{22} = A_{11}$, for which case the bracket $(.5b_2c_2-.5b_1c_1)$. in the denominator will also be zero.

ii) The surface area correlation factor, AF, is simply the ratio of the fin areas,

$$AF = \frac{A_1}{A_2} \tag{8b}$$

The reverse order of A_2 to A_1 is logical since if A_2 is larger than A_1, one would expect the lift losses to be smaller. This would be due to the contribution of lift produced by A_{20}, which should be affected very little by the gap which dominates the lower area of A_{22}.

iii) The gap height correlation factor, GF, was found to be:

$$GF = \left(\frac{(g/D)_1}{(g/D)_2}\right)^{\left[1.6 - \left(\frac{(g/D)_1}{(g/D)_2}\right) \cdot \left(\frac{(g/D)_2 - .04}{.05}\right)\right]^{-1}} \tag{8c}$$

where if $(g/D)_2 = 0.04$, GF will be simply

$$GF = \{(g/D)_1/(g/D)_2\}^{1/1.6}$$

One should note that the correlation employs the gap to diameter ratio rather than the absolute gap height only.

iv) The chord/span factor, CSF, was found to be in the form:

$$CSF = \sqrt{\left(\frac{b_2}{b_1}\right)\left(\frac{c_2}{c_1}\right)} \tag{8d}$$

where b_2 and b_1 are not, in general, equal to the semi-span heights, but rather the top apex heights for the triangular areas A_{22} and A_{11} respectively. This can be shown if Figure 8 is considered and the concept is applied to the many planforms of Figure 9. For many fin planforms however, b_2 and b_1 can be the same as the fin semi-spans.

v) The boundary layer factor, BF, was based on the boundary layer thickness at the leading edge of the fin at the fin root section. It was found appropriate to write:

$$BF = (\delta_{LE2}/\delta_{LE1})^{.88} \tag{8e}$$

where the boundary layer thickness, δ_{LE}, was estimated by the familiar form[17] for turbulent boundary layers in axisymmetric tubes:

$$\delta_{LE1} = .37\, X_{LE1} / \left(R_{e_{X_{LE1}}}\right)^{.2}$$

Finally, one summarizes the fin normal force loss correlation factor as

$$FNF_2 = \left.\frac{C_{N_{\alpha fg}}}{C_{N_{\alpha f}}}\right|_2 = \left[\left\{\frac{\left(\frac{.76A_{20}+A_{22}}{A_{22}}\right)+\left(\frac{.24A_{20}(A_{22}-A_{11})}{(.5b_2c_2)(.5b_2c_2-.5b_1c_1)}\right)}{\left(\frac{.76A_{10}+A_{11}}{A_{11}}\right)+\left(\frac{.24A_{10}(A_{22}-A_{11})}{(.5b_1c_1)(.5b_2c_2-.5b_1c_1)}\right)}\right\}\cdot\left\{\frac{A_1}{A_2}\right\}\cdot\left\{\frac{(g/D)_1}{(g/D)_2}\sqrt{\frac{1.6-\left(\frac{(g/D)_1}{(g/D)_2}\right)\left(\frac{(g/D)_2-.04}{.05}\right)}{1}}\right\}\cdot\left\{\sqrt{\left(\frac{b_2}{b_1}\right)\left(\frac{c_2}{c_1}\right)}\right\}\cdot\left\{\left(\frac{\delta_{LE2}}{\delta_{LE1}}\right)^{.88}\right\}\right] \cdot \left.\frac{C_{N_{\alpha fg}}}{C_{N_{\alpha f}}}\right|_1$$

$$= CF \cdot FNF_1 \qquad (9)$$

which can be used to predict the losses for a new fin, 2, based on the known losses of another totally different fin ,1, under totally different flow conditions.

For the direct prediction of losses for any fin, it was decided that the triangular fin of Dahlke & Pettis would be used at g/D = .06, as the reference known case. This choice was made in order that future corrections to the analysis of Bleviss and Struble would be applicable to that configuration. Knowing the geometric data of that reference fin and its normal fin loss factor, the prediction of $\left(C_{N_{\alpha fg}}/C_{N_{\alpha f}}\right)_2$ for any fin should be made using the equation

$$\left.\frac{C_{N_{\alpha fg}}}{C_{N_{\alpha f}}}\right|_2 = \left[\left\{\frac{\left(\frac{.76A_{20}+A_{22}}{A_{22}}\right)+\left(\frac{.24A_{20}(A_{22}-.3675)}{(.5b_2c_2)(.5b_2c_2-.3675)}\right)}{1}\right\}\cdot\left\{\frac{.3675}{A_2}\right\}\cdot\left\{\left(\frac{.06}{(g/D)_2}\right)\sqrt{\frac{1.6-\left(\frac{.06}{(g/D)_2}\right)\left(\frac{(g/D)_2-.04}{.05}\right)}{1}}\right\}\cdot\left\{\sqrt{\left(\frac{b_2}{.525}\right)\left(\frac{c_2}{1.4}\right)}\right\}\cdot\left\{\left(\frac{\delta_{LE2}}{.1934}\right)^{.88}\right\}\right] = .795 \qquad (10a)$$

where the lengths b_2, c_2, δ_{LE2} are in inches and the areas A_{20}, A_{22}, A_2 are in $(inch)^2$. For SI units, the same relation can be easily re-written as

$$\left.\frac{C_{N_{\alpha fg}}}{C_{N_{\alpha f}}}\right|_2 = \left[\left\{\frac{\left(\frac{.76A_{20}+A_{22}}{A_{22}}\right)+\left(\frac{.24A_{20}(A_{22}-237.09)}{(.5b_2c_2)(.5b_2c_2-237.09)}\right)}{1}\right\}\cdot\left\{\frac{237.09}{A_2}\right\}\cdot\left\{\left(\frac{.06}{(g/D)_2}\right)\sqrt{\frac{1.6-\left(\frac{.06}{(g/D)_2}\right)\left(\frac{(g/D)_2-.04}{.05}\right)}{1}}\right\}\cdot\left\{\sqrt{\left(\frac{b_2}{13.33}\right)\left(\frac{c_2}{35.56}\right)}\right\}\cdot\left\{\left(\frac{\delta_{LE2}}{4.912}\right)^{.88}\right\}\right] = .795 \qquad (10b)$$

where the lengths b_2, c_2, δ_{LE2} are in mm and the areas A_{20}, A_{22}, A_2 are in $(mm)^2$.

2. SLOT EFFECTS

Only effects on the fin normal force are considered. The effects on axial forces were discussed in Reference 15 but they are not considered in this work. The approach used here is that of Washington et al[13,14] and which is briefly summarized. The carry over lift factor, $K_{B(T)}$, of Equation 1 which represents the increase in body lift due to the presence of the fin, is eliminated. That is to say, with the existence of a slot at or near the fin root chord, the contribution of the fin to the body lift is negligible. Washington et al,[13] showed that this approach yielded the observed normal force loss measured in the wind tunnel. The results were shown to be good for small α ($< \pm 6°$) but were shown only for subsonic speeds (M = 0.5-.95). Because the analysis was based on slender body theory (independent of Mach number), that approach was applied here up to Mach number 1.2 . Based on physical considerations one should expect a lesser effect of slots at higher supersonic speeds. Therefore, that approach might not be applicable in the high supersonic speed regime. Another point to be made is that this approach does not account for slot location, shape, area, or depth. It would have been helpful if experimental data were available for those specific areas of interest.

III. RESULTS

1. GAP EFFECTS

a. Validation of the gap model Fifteen cases of validation of Equation (9) were made using the four data sets for gaps.[6-9] Cross correlations were made for every shape, aspect ratio, gap height, body diameter and Reynolds number. All the case designation numbers are given in Figure 12. The baseline case, as referred to earlier, is the triangular fin shape of Dahlke et al with g/D = .06 . The results using that correlation, with reference to Killough's two cases of AR = 1.0 and 3.0 are given in Figures 13a and 13b. The prediction is shown to be very good. The results of the application of Equation (9) to another two fin cases of Dahlke et al, of AR = 0.5 and 1.0, are shown in Figure 14 where the agreement is excellent. The results of applying Equation (9) to the single fin shape of Henderson is given in Figure 15 and the predicted value is shown. It should be mentioned that the single case of Henderson showed large disagreement with those of Dahlke et al, which are more uniform and more trust-worthy, as indicated in Henderson's report.[8] Application of Equation (9) to the case of Fellows at M = .8 for a fin of AR = 2.22 gave good result as shown in Figure 16. The data point at M = .6 is beyond the intended Mach range, and it shows a value close to .977. However, this single data point cannot be used to establish a model which is for the subsonic regime of M < .7 . The trend of this result at M = .6 agrees with the trend postulated and shown in Figure 11 where a sudden rise in the value of FNF is expected towards M = 0. The remainder of the fifteen cases are not shown plotted. However, the results are all given in Table 1, along with comparisons with the deduced wind tunnel results. The case designation numbers appearing in Table 1 were given earlier in Figure 12.

TABLE 1. Results of the Present Analysis for Fifteen Test Cases.

Correlation Case No.	The Correlation Factor (CF)		Fin Normal Force Reduction Factor (FNF)	
	Prediction Eq. (8)	Wind Tunnel	Prediction Eq. (9)	Wind Tunnel
1	1.045	1.04	.831	.826
2	1.114	1.07	.886	.851
3	1.069	1.03	.883	.851
4	0.99	0.956	.787	.760
5	1.225*	1.132*	.974*	.90*
6	1.213*	1.184*	.922*	.90*
7	1.05	1.09	.800	.826
8	0.91*	0.945*	.819*	.851*
9	1.153*	1.09*	.952*	.90*
10	1.093	1.12	.831	.851
11	1.053	0.986	.837	.784
12	1.007	1.03	.765	.784
13	0.86	0.871	.774	.784
14	1.131	1.198	.900	.953
15	1.169	1.226	.929	.975

*These cases involved a very low aspect ratio fin where the estimated boundary layer thickness was 55% of the fin height.

b. Application to the Copperhead projectile The configuration consisting of body and tail fins was considered. The Copperhead tail fin gap is .02 inch (5 mm) as shown in Figure 2. The g/D ratio is .033. However, the existance of the slot ahead of the tail fin, as can be seen in Figure 1, and the slot flow into the body as seen in Figure 9, might cause the "effective" gap height to be quite different than the physical one. Therefore the application of the present gap model can be considered to provide only an estimate rather than an actual value. One might either increase or decrease the "g" height to account for this diffusion; but this variation would be highly arbitrary and cannot be used formally without good justification. Therefore, in the present application, only the true physical value of .02

inch (5 mm) was used. Of course, the larger the effective gap, the larger the normal force loss would be. One other peculiarity to be considered in the case of the Copperhead is the gap blockage or "fin stem interference". As can be seen from Figure 19a, the tail fin stem is quite bulky and is twice the width of the maximum fin root thickness. This added blockage is certain to reduce the estimated gap losses. All the data used to formulate the present correlation includes a small fin stem interference effect, but not for such an unusual blockage. Therefore, it is expected that the present model will predict larger gap losses than those actually incurred for the case of the Copperhead projectile.

The normal force slope coefficient with gap effects is given in Figure 17. The Missile Datcom Code was used to provide the no-gap case and the modification for the gaps were made using Equations (4) and (9). The modification was made over the extended Mach range of $0.8 \leq M \leq 1.6$.

The pitching moment slope coefficient with gap effects is shown in Figure 18, and was obtained by the same method. However, there were no corrections for the location of center of pressure for the fin load with gaps. This correction should and will be considered in future efforts.

2. SLOT EFFECTS: APPLICATION TO THE COPPERHEAD PROJECTILE

The same configuration of body and tail fins was considered. The slots of Figure 19a were modeled using Washington's approach.[13] The corrected normal force slope coefficient is given in Figure 20. As mentioned earlier, that approach is Mach number independent, therefore the application here was made over the Mach range $0.5 \leq M \leq 1.8$. As in previous predictions, the DATCOM code results were modified accordingly to provide the new results. The corresponding pitching moment slope coefficient is given in Figure 21, and was obtained by the same method outlined before.

3. COMBINED GAP AND SLOT EFFECTS

The normal force losses due to gaps and slots were combined and the computed normal force slope coefficient is given in Figure 20 over the extended range $0.8 \leq M \leq 1.6$. The reduction of C_{N_α} was about 21% near Mach 1.05.

The corresponding pitching moment slope coefficient, C_{M_α}, is shown in Figure 23 for the combined effects of gaps and slots. The reduction of C_{M_α} was 38% near $M = 1.05$. It is felt that with proper consideration of the movement of the location of the center of pressure of the tail fin due to gaps and slots, C_{M_α} would be better predicted.

In the free flight firing tests, the projectile is spinning at a moderate rate where the slot and gap effects may differ significantly from those observed in the wind tunnel. This explanation may be used to interpret the large differences noticed between wind tunnel and firing test data. One should therefore expect that the present predictions to be, in general, closer

to the wind tunnel data than to those of the firing range data. This is due to the controlled environment of the wind tunnel, and its nonspinning conditions.

IV. CONCLUSIONS

All existing data covering fin-body gap and body slot effects have been surveyed, analyzed and utilized. A correlation relation was established to provide the magnitude of the normal force losses of fins due to streamwise fin-body gap for any fin shape and gap size, in the transonic speed regime of $0.8 < M < 1.2$. Existing data also supports the validity of the correlation in the wider range of $0.7 < M < 1.8$ without noticeable loss in accuracy. The established correlation is based on all the experimental data surveyed and has been validated over 15 different cases with accuracy of ±5%. This correlation takes into account the variations in fin shape, fin area, fin span and chord lengths, gap height, body diameter, and Reynolds number. The correlation is highly useful for including viscosity and fin support effects which are included in the correlation. This approach has advantages over existing inviscid analyses which cannot be used for small gaps where viscosity effects dominate, nor do they account for the fin support interference. The correlation is in algebraic form and uses direct, measurable fin geometry and flight condition inputs. It is simple, and can be used in any of the fast aerodynamic prediction codes for practical fin design purposes.

Body slot effects on reducing the fin normal force losses were modeled using a previously suggested model.[13] That model was validated in the subsonic speed regime only, although the theory behind it allows it to be used also in supersonic speeds for slender bodies. This model, however, does not account for the slot shape, area, depth or location relative to the fin. The model is simple and can be directly used in the fast design codes as well. Both models are valid for small angles of attack, usually considered to be in the range $\alpha < \pm 6°$.

An application was made of these two models to the geometry of the Copperhead Guided Projectile. That configuration, with very large fin stem and deep slot flow is not a typical configuration for application of both models. However, the results obtained using those models have shown a reduction of the total normal force and pitching moment by values as large as 21% and 38%, respectively. Comparison with wind tunnel and range results showed improved agreement.

Although all the data used in the present analysis was based on a body with four cruciform fins, the analysis should be useful for any set of fins with arbitrary number of blades (< 8), for small angles of attack.

Future improvements should include: 1) the correction to the location of the center of pressure of the fin with gaps or slots. This correction will not affect the normal force, but rather the pitching moment; 2) representing an equivalent streamwise gap height (or gap area) to account for nonstreamwise gaps which occur when the control surface is deflected at an angle relative to the body axis. This latter effect is very important for all missiles and projectiles with controllable lifting surfaces. A study for this suggested latter improvement has started and will be reported, after validation, in the future.

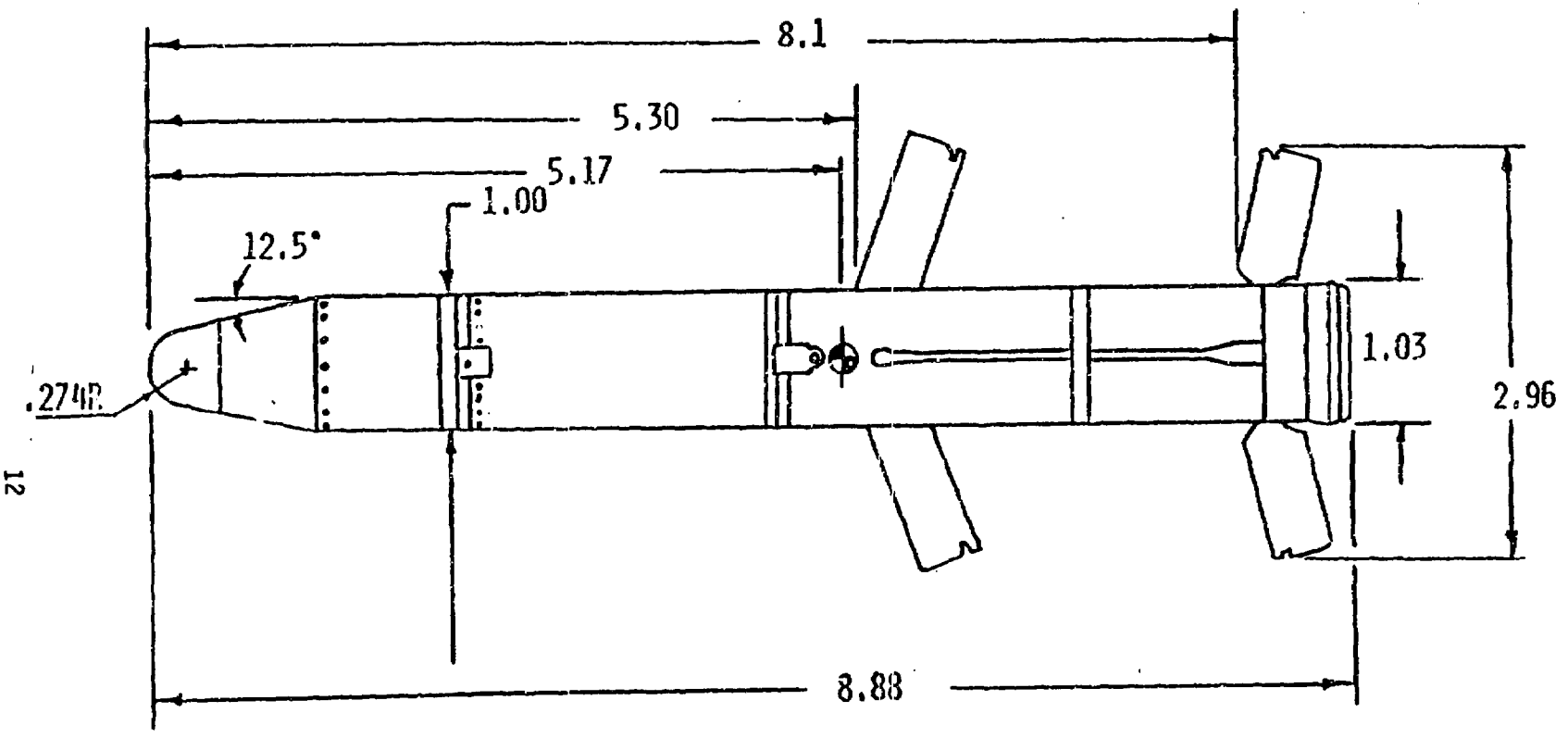

Figure 1. Configuration of the Copperhead projectile.

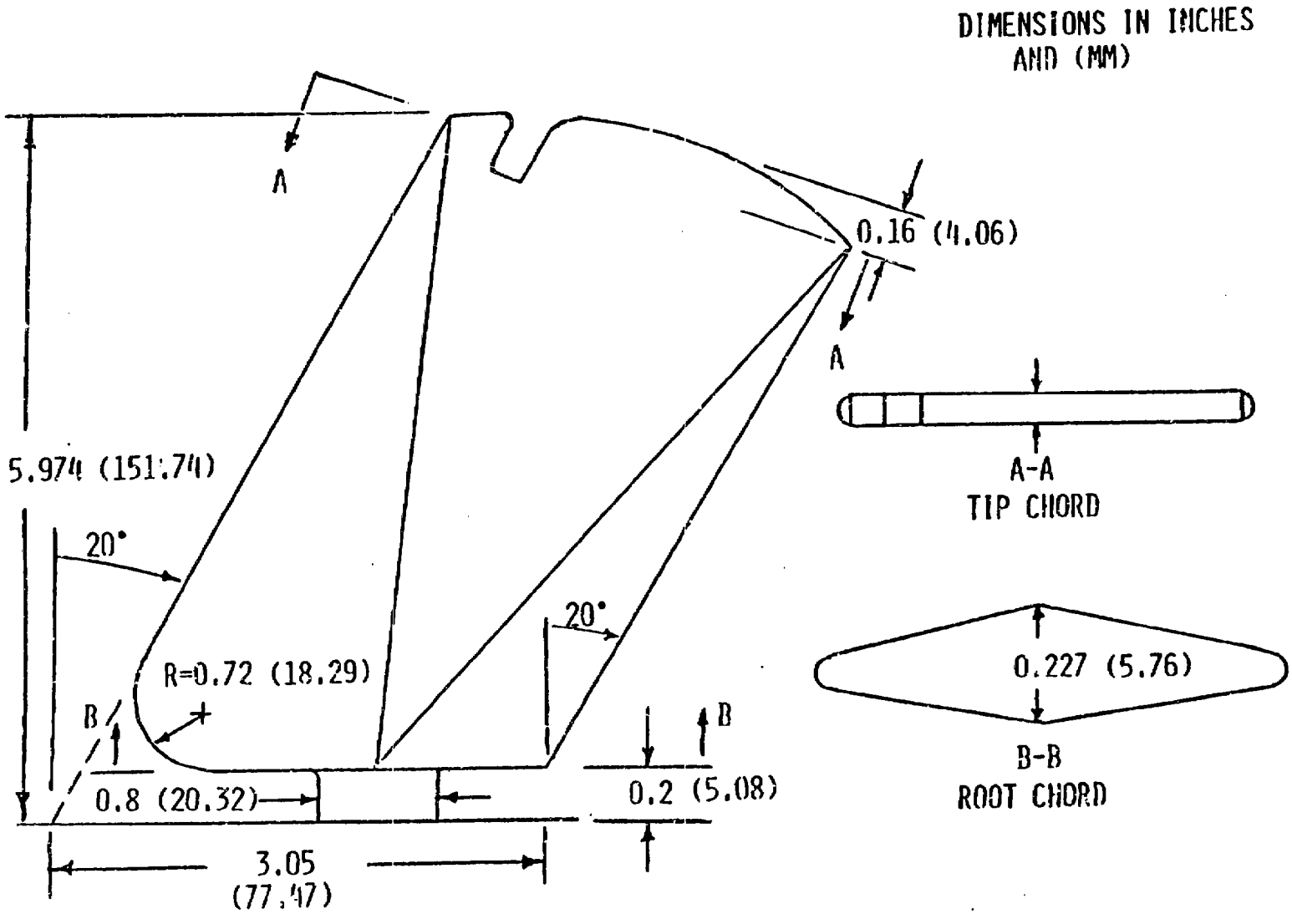

Figure 2. Copperhead tail fin and gap configuration.

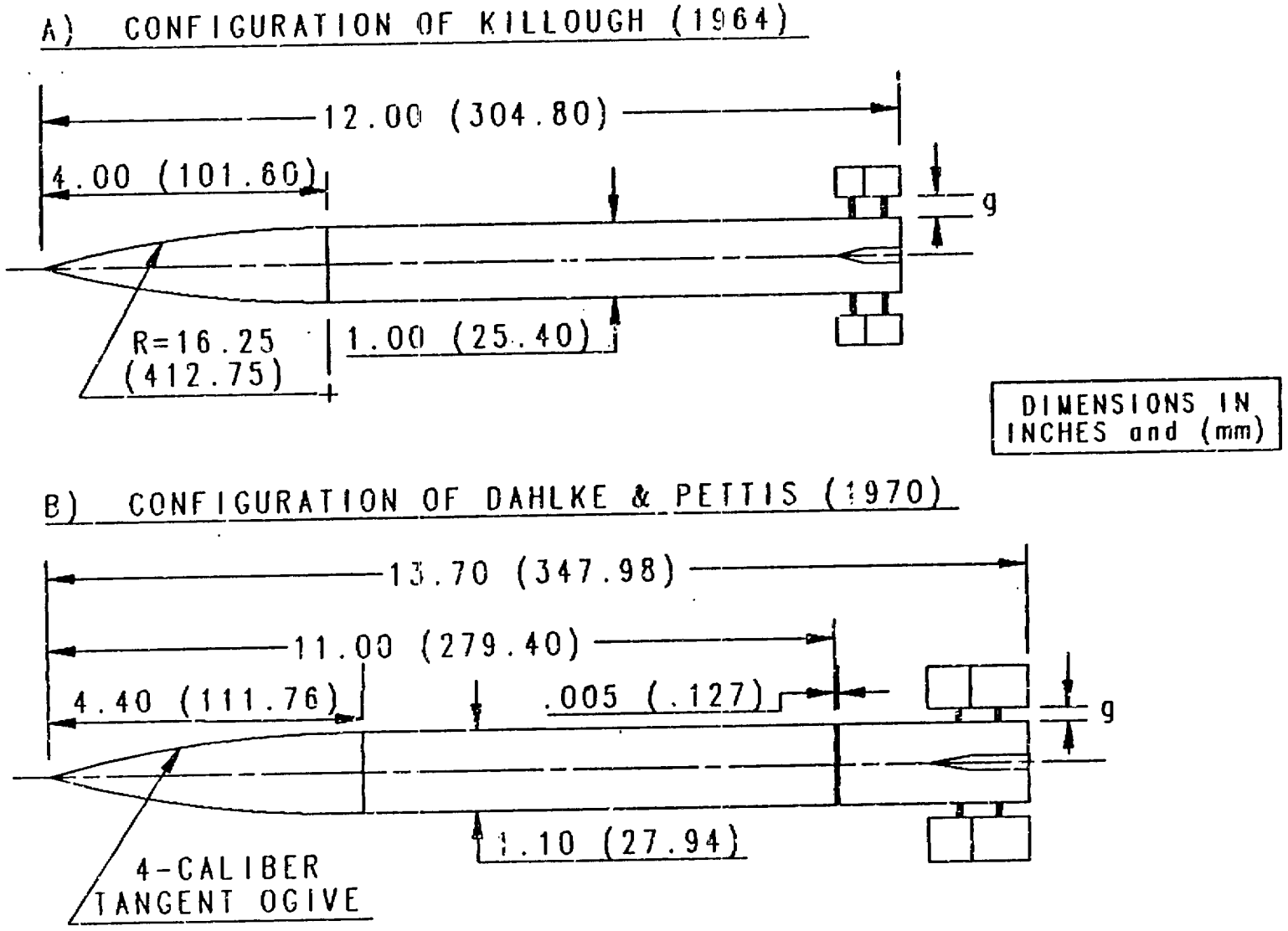

Figure 3. Wind tunnel model configurations.

C) CONFIGURATION OF HENDERSON (1977)

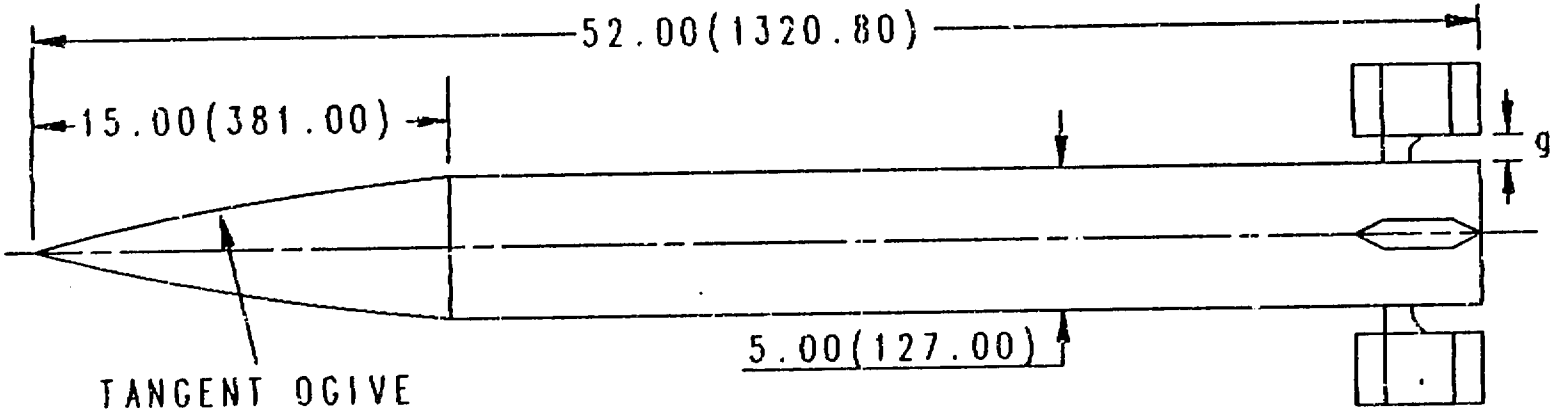

D) CONFIGURATION OF FELLOWS (1982)

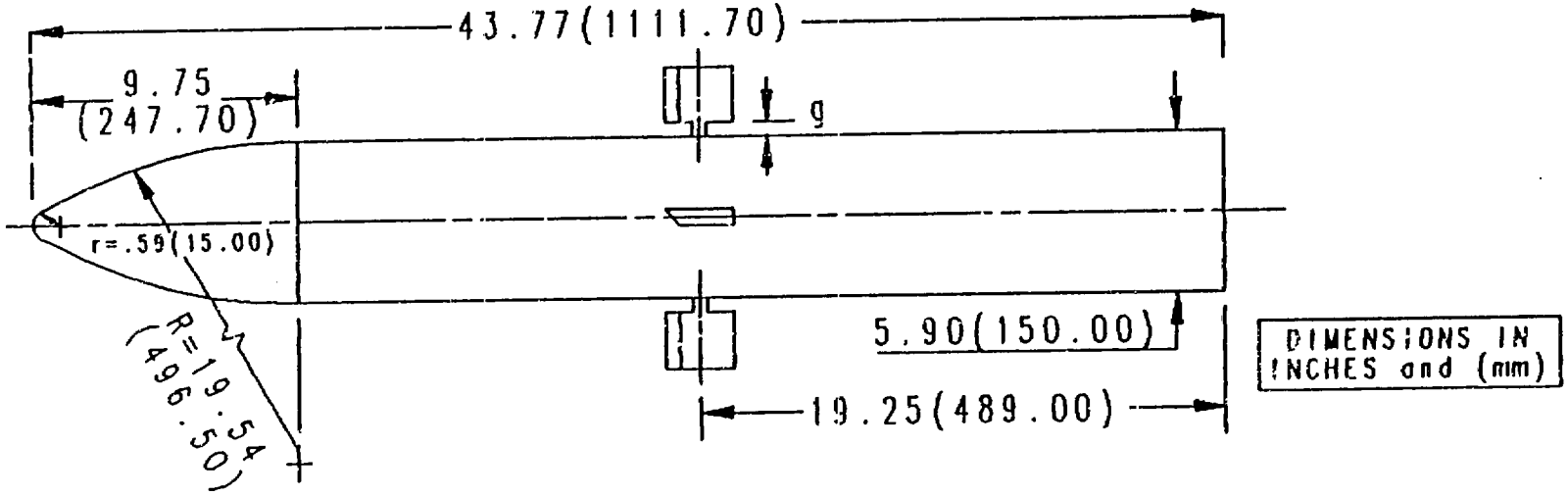

Figure 4. Wind tunnel model configurations.

A) FIN CONFIGURATIONS OF KILLOUGH (1964.)

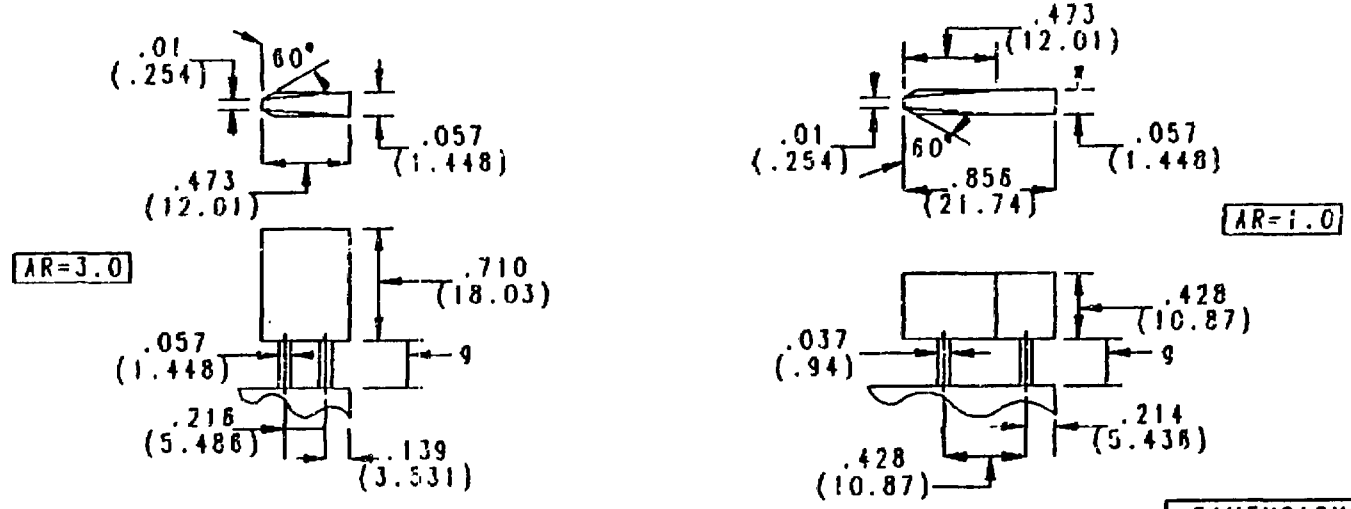

B) FIN CONFIGURATIONS OF DAHLKE & PETTIS (1970)

DIMENSIONS IN INCHES and (mm)

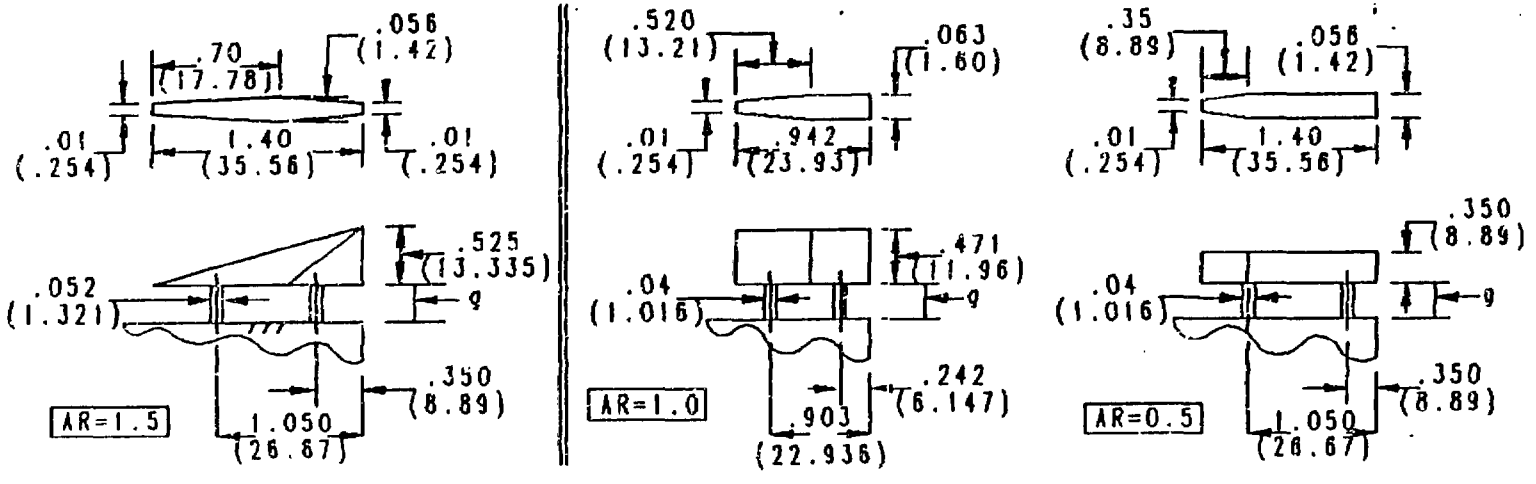

Figure 5. Details of fin panel configurations.

C) FIN CONFIGURATION OF HENDERSON (1977)

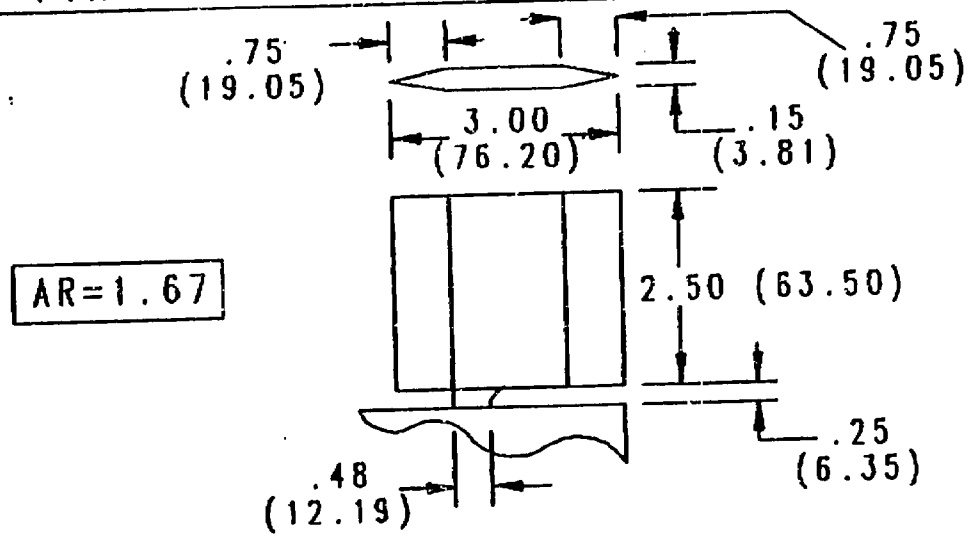

DIMENSIONS IN INCHES and (mm)

D) FIN CONFIGURATIONS OF FELLOWS (1982)

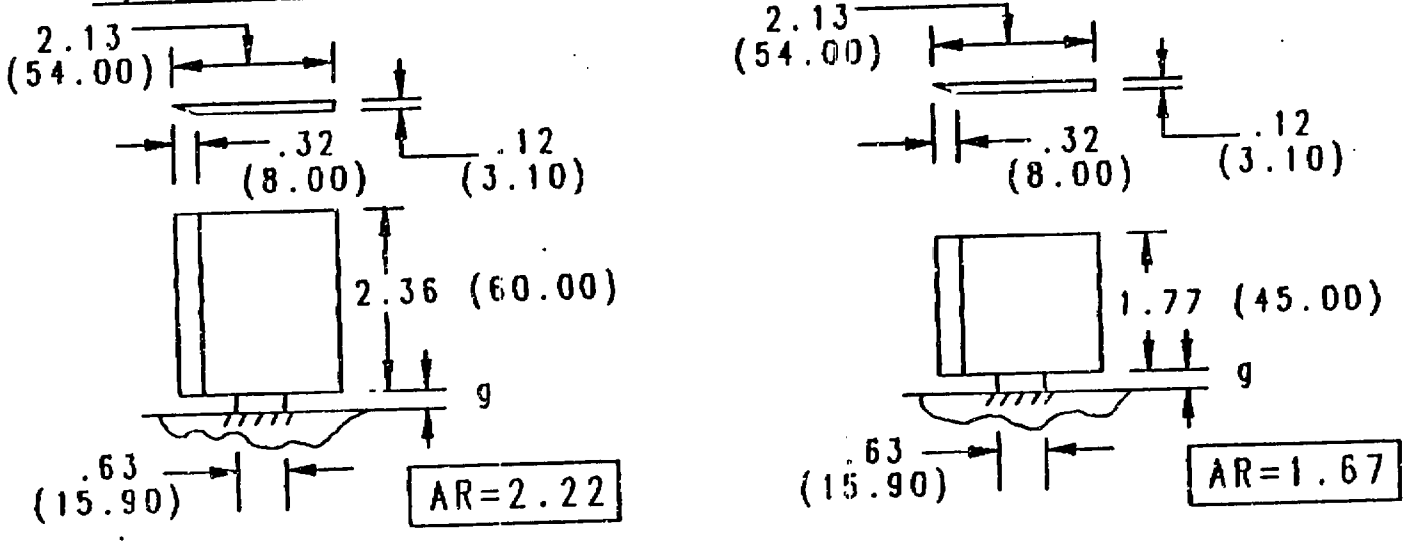

Figure 6. Details of fin panel configurations.

Killough's Data (1964)

D = 1.0" (25.4)

M = .8 to 4.5

R_e = .4 x 10^6 per inch
(.157 x 10^6 per cm)

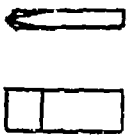

AR = 1.0 Af = .3663	AR = 2.0 Af = .3364	AR = 3.0 Af = .3358
g/D-(Ag/Af)	g/D-(Ag/Af)	g/D-(Ag/Af)
0.0 - (0.0)	0.0 - (0.0)	0.0 - (0.0)
0.08-(.187)	0.08-(.138)	0.08-(.113)
0.16-(.374)	0.16-(.276)	
0.25-(.584)	0.25-(.430)	

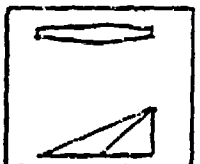

AR = 1.5 Af = .3675	AR = 0.5 Af = .490	AR = 0.75 Af = .7350	AR = 1.0 Af = .4437
g/D-(Ag/Af)	g/d-(Ag/Af)	g/D-(Ag/Af)	g/D-(Ag/Af)
0.00-(0.0)	0.00-(0.0)	0.00-(0.0)	0.00-(0.0)
0.06-(.251)	0.06-(.188)	0.06-(.126)	0.08-(.187)
0.12-(.502)	0.12-(.377)	0.12-(.251)	0.16-(.374)
0.20-(.837)	0.20-(.638)	0.20-(.419)	0.25-(.584)

Dahlke & Pettis' Data (1970)

D = 1.1" (27.94)

M = .8 to 4.5

R_e = .415 x 10^6 per inch
(.163 x 10^6 per cm)

Henderson's Data (1977)

D = 5.0" (127.)

M = .7 to 1.2

R_e = .316 x 10^6 per inch
(.124 x 10^6 per cm)

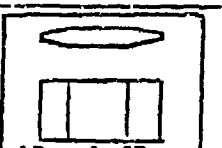

AR = 1.67 Af = 7.500
g/D-(Ag/Af)
0.0-(0.0)
0.5-(.10)

Fellows' Data (1982)

D = 5.905" (150.)

M = 0.6 and .85

R_e = .287 x 10^6 per inch (M = .6)
(.113 x 10^6 per cm)
.340 x 10^6 per inch (M = .85)
(.134 x 10^6 per cm)

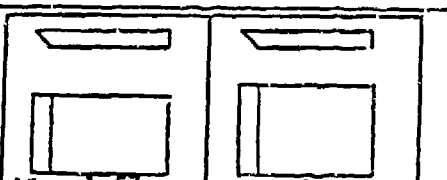

AR = 1.67 Af = 3.767	AR = 2.22 Af = 5.022
g/D-(Ag/Af)	g/D-(Ag/Af)
0.0-(0.0)	0.0-(0.0)
0.02-(0.66)	.02-(.050)

DIMENSIONS IN INCHES & AREAS ARE IN $(INCH)^2$
1 INCH = 25.4 mm 1 $(IN)^2$ = 645.16 $(mm)^2$

Figure 7. Test conditions for all known data utilized.

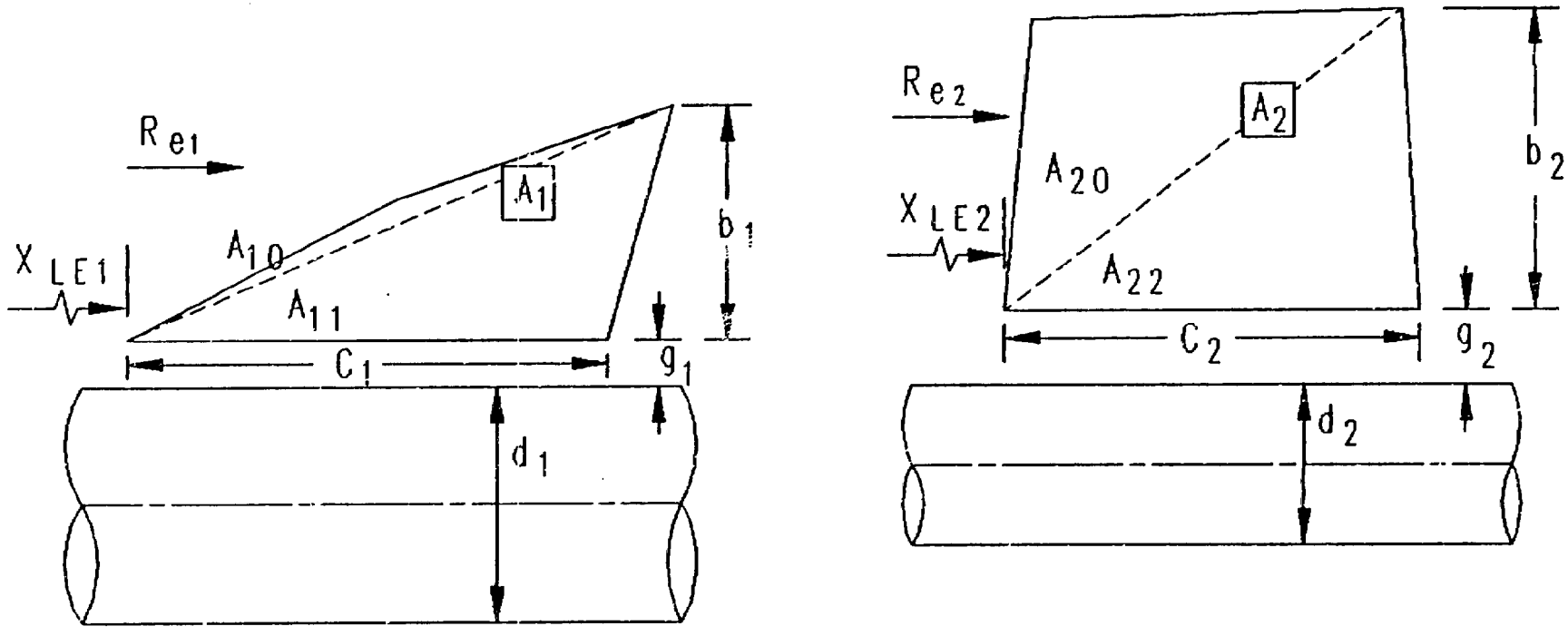

Figure 8. Nomenclature for the correlation analysis.

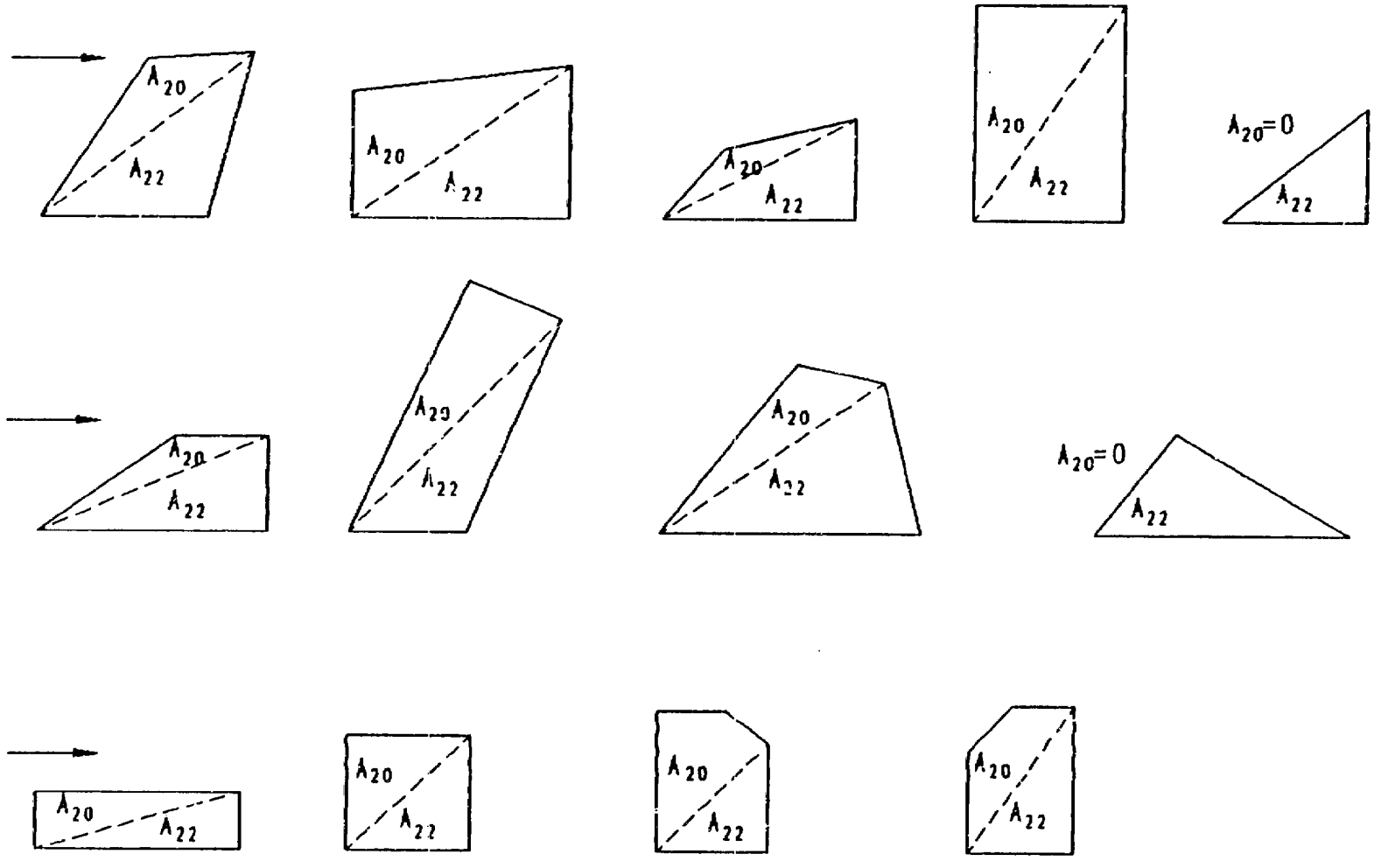

Figure 9. Examples of fin area desgination for several fin planforms.

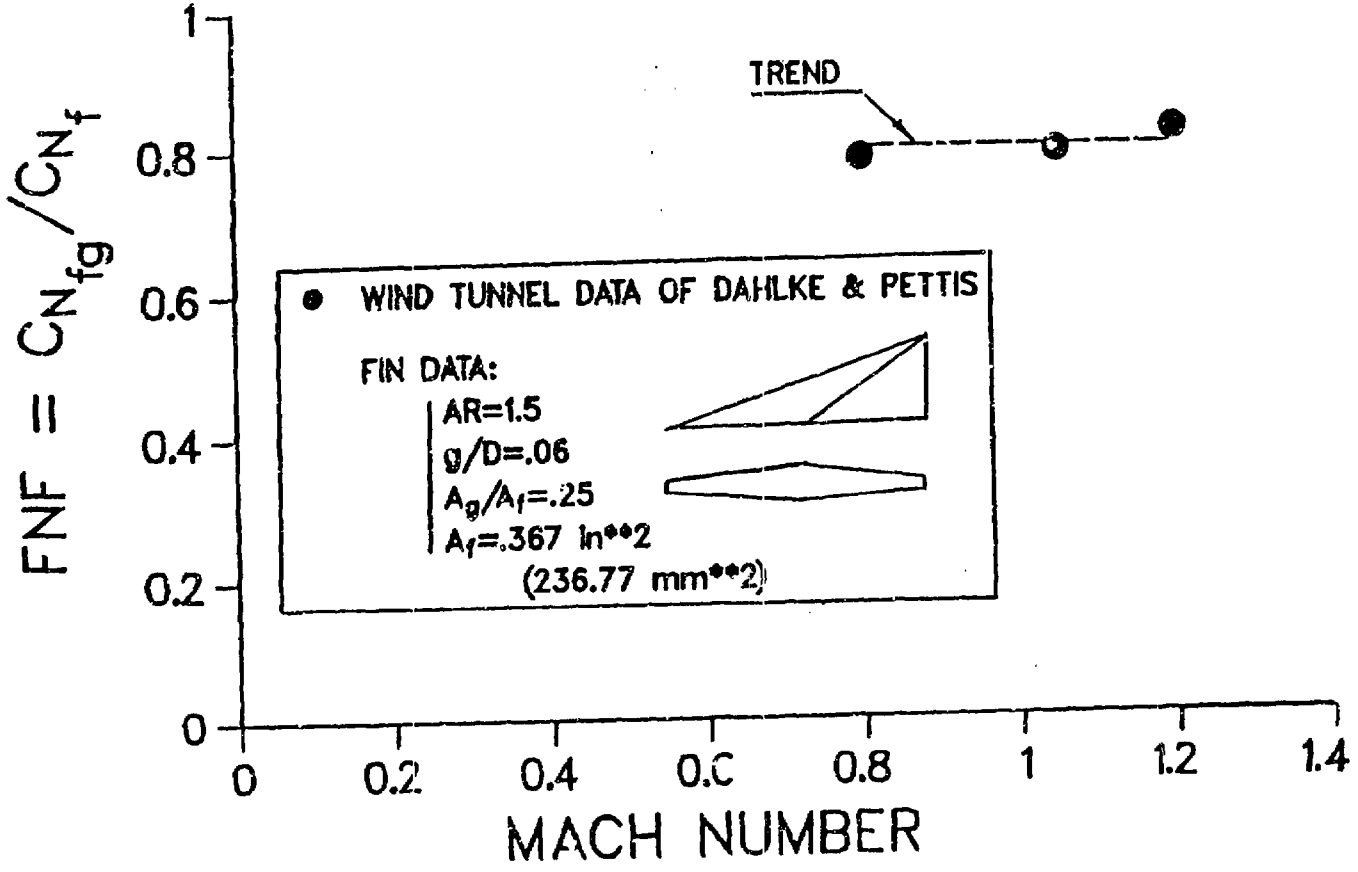

Figure 10. Transonic wind tunnel data for triangular fin of AR = 1.5.

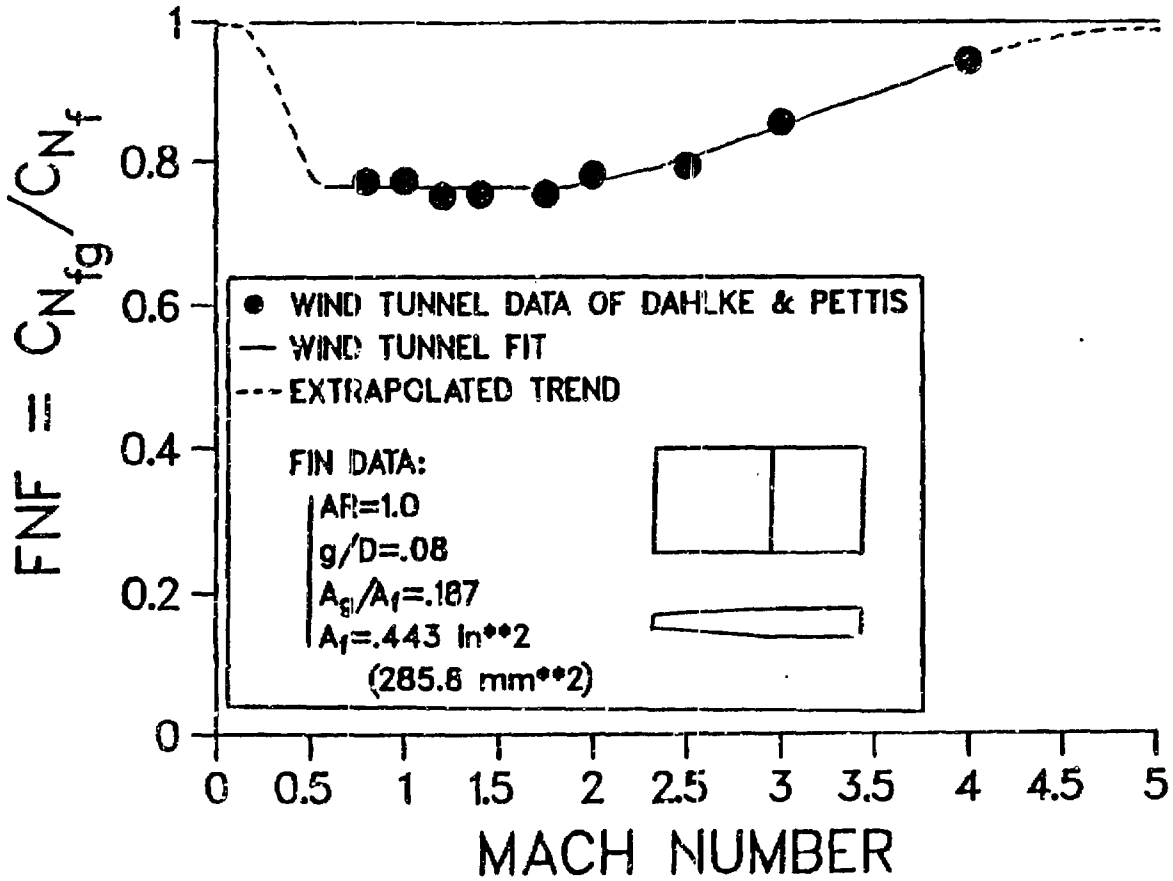

Figure 11. Wind tunnel data for rectangular fin of AR = 1.0.

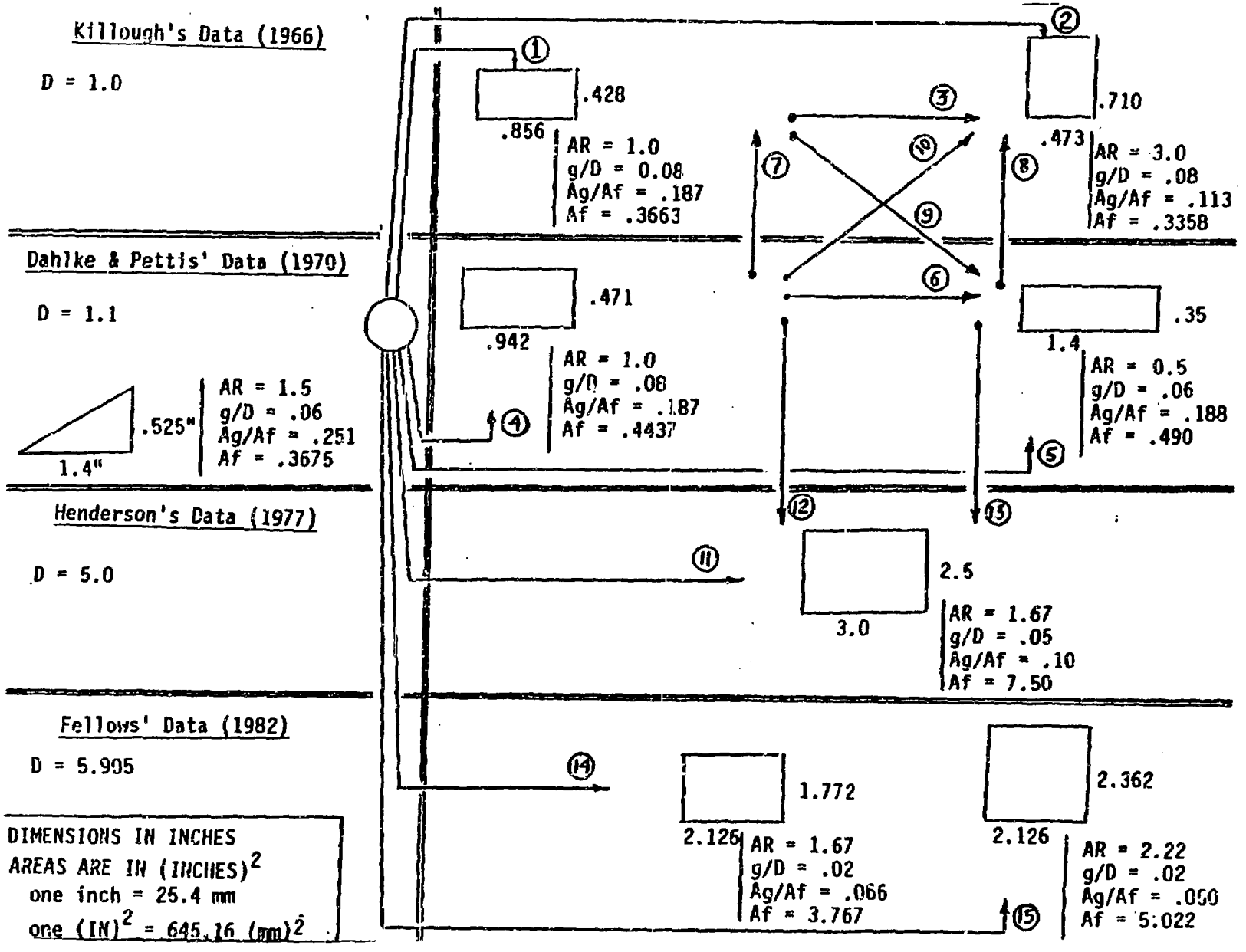

Figure 12. Case designation for fifteen correlation tests used for validation.

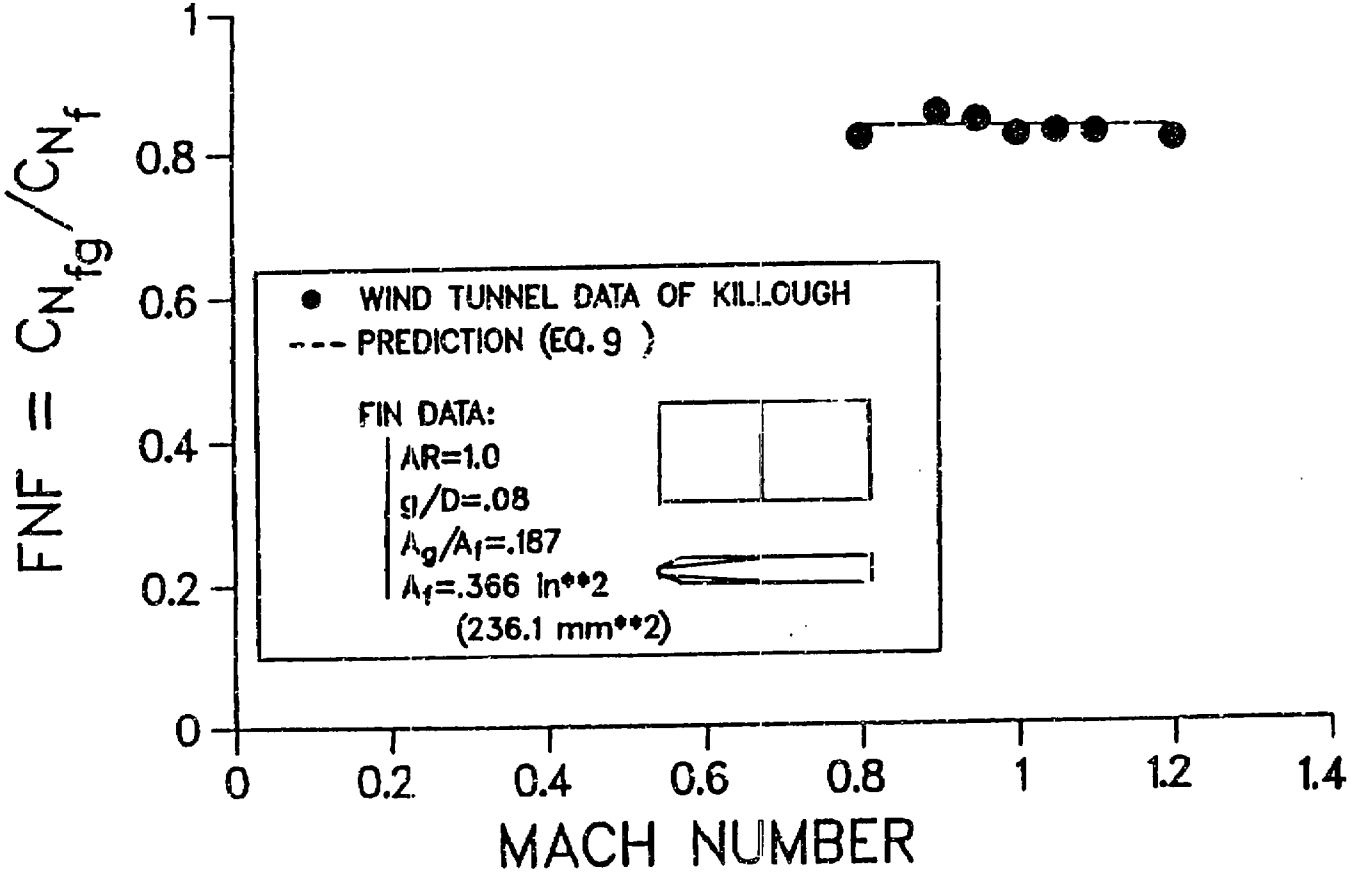

Figure 13a. Comparison with data of Killough, rectangular fin of AR = 1.0.

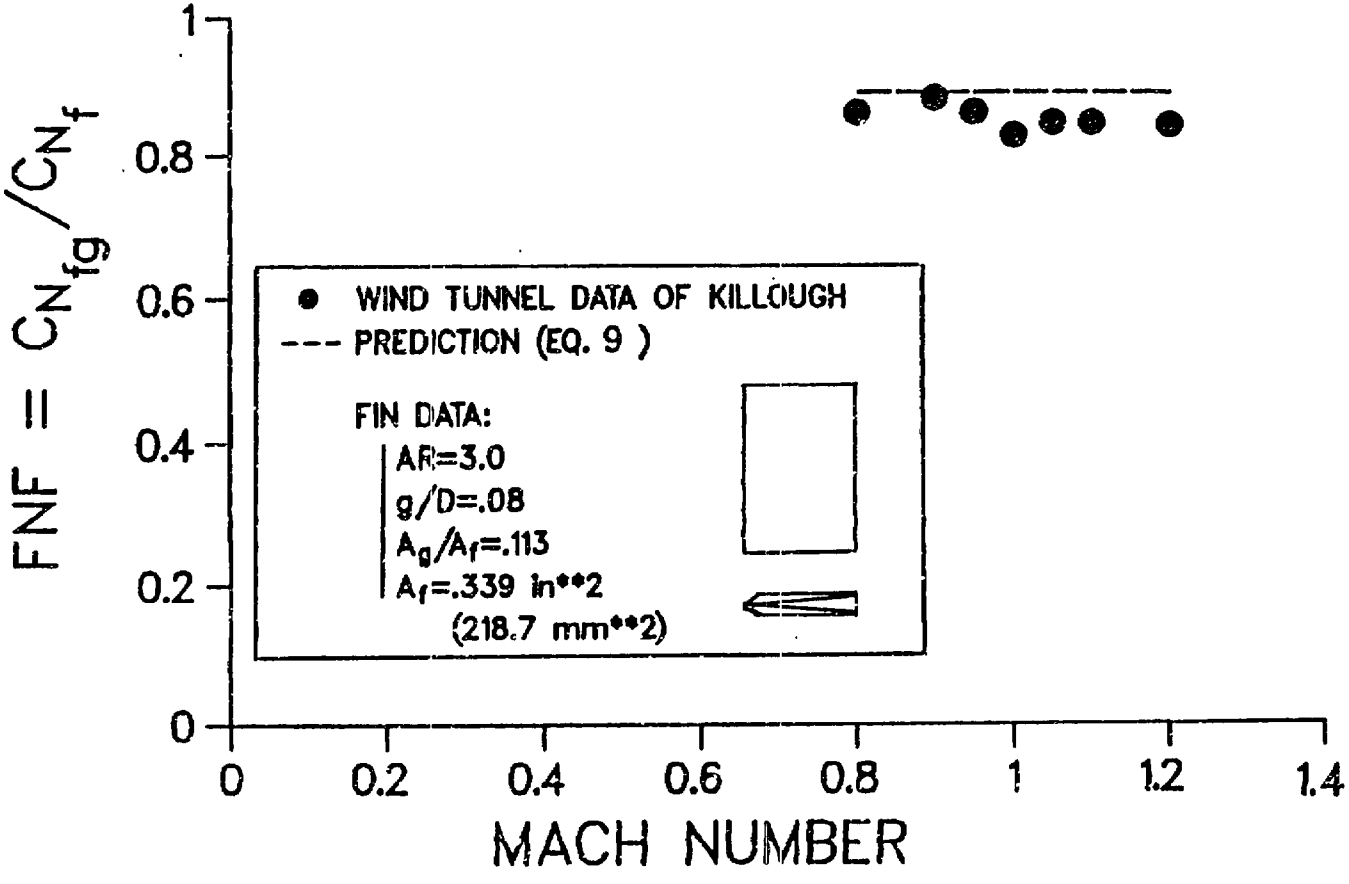

Figure 13b. Comparison with data of Killough, rectangular fin of AR = 3.0.

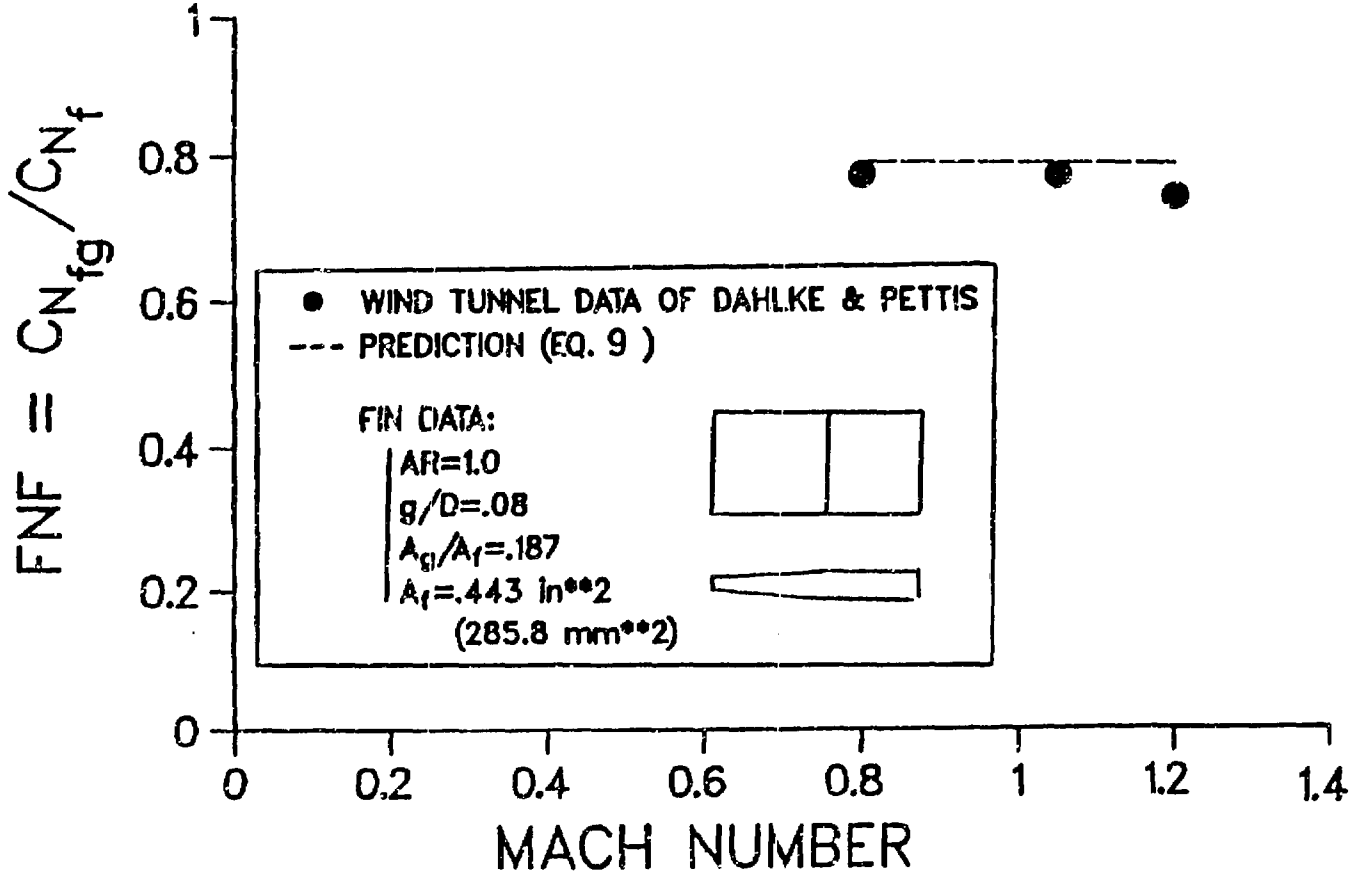

Figure 14a. Comparison with data of Dahlke and Pettis, rectangular fin of AR = 1.0.

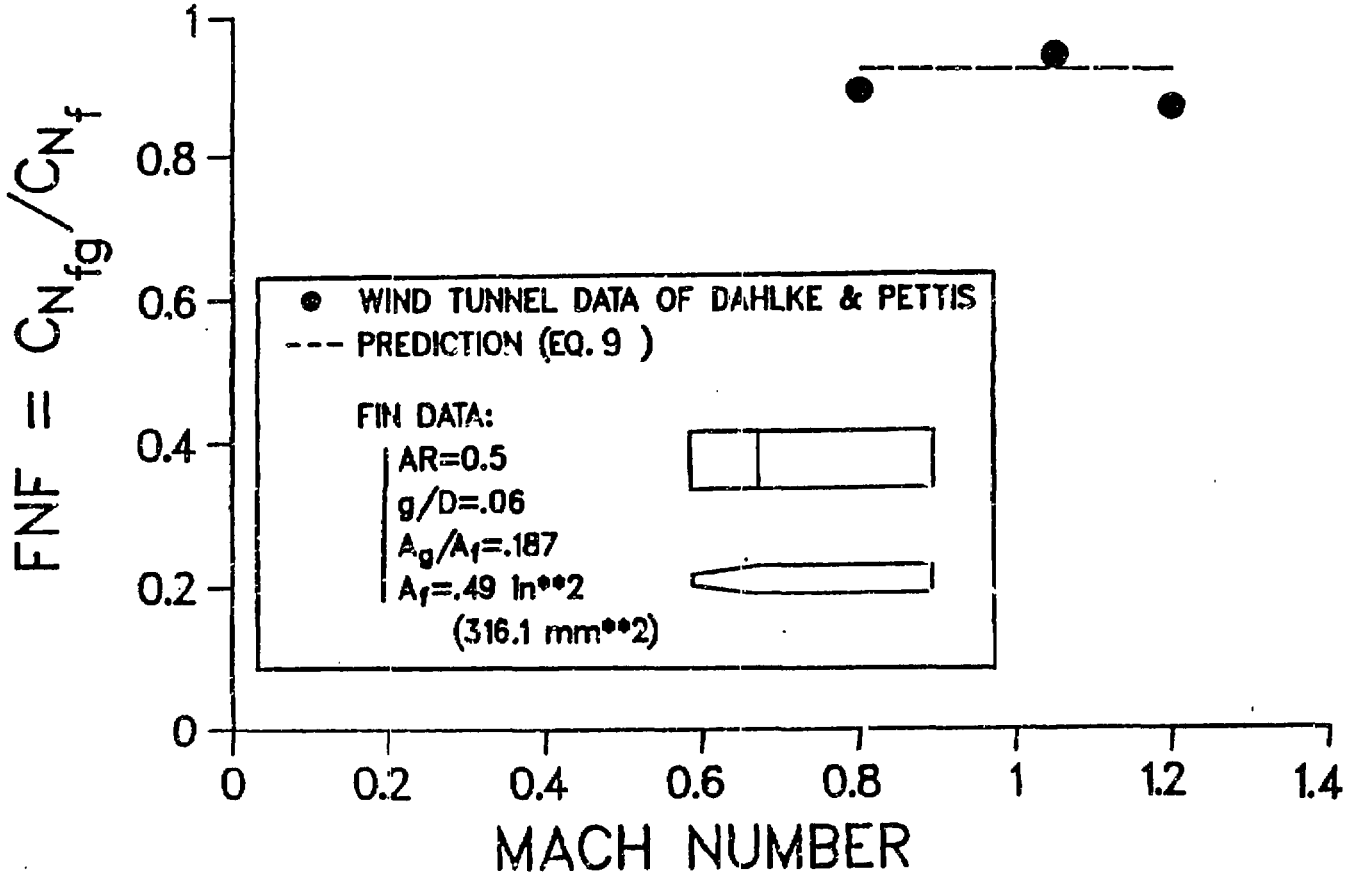

Figure 14b. Comparison with data of Dahlke and Pettis, rectangular fin of AR = 0.5.

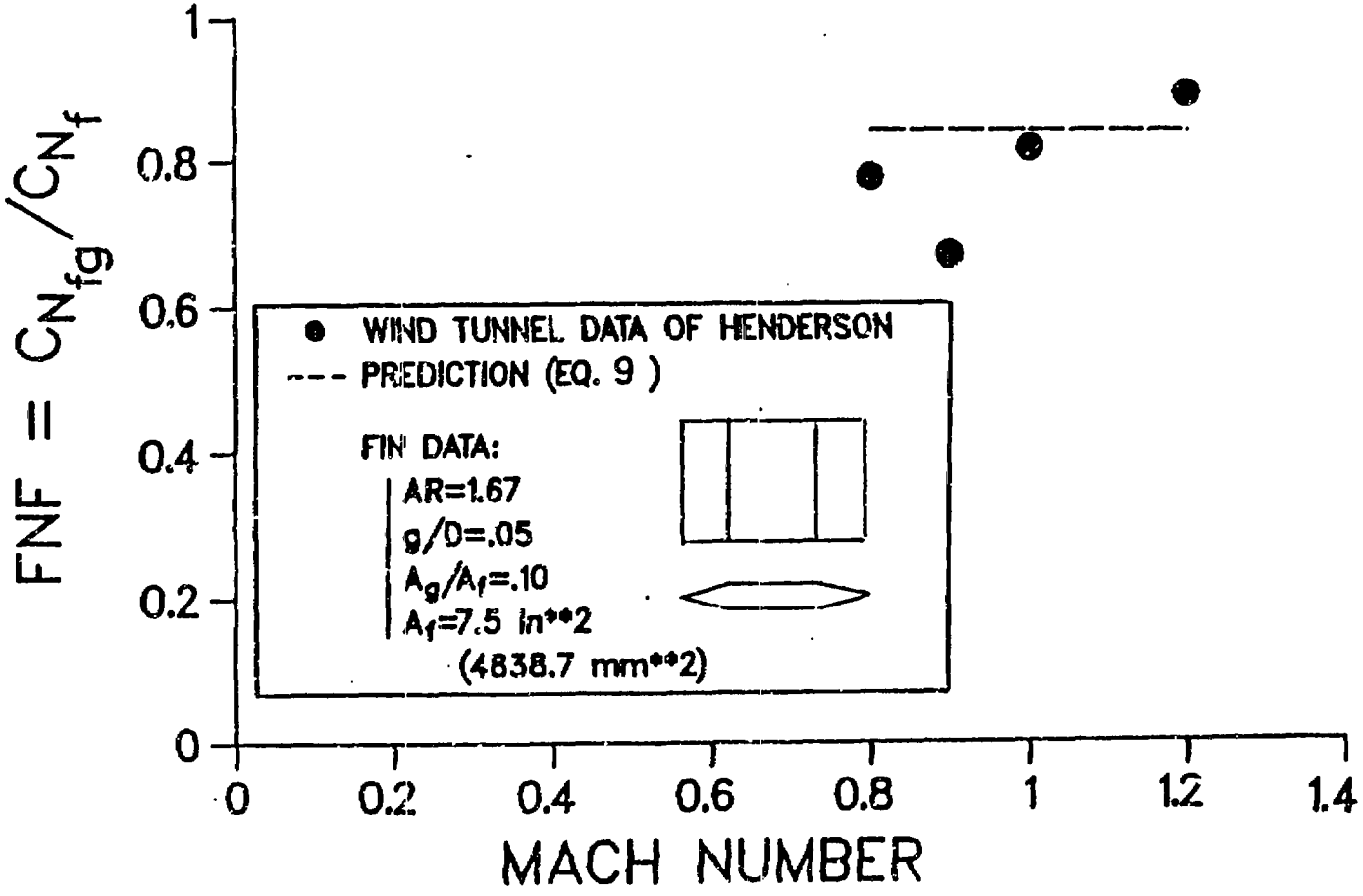

Figure 15. Comparison with data of Henderson, rectangular fin of AR = 1.671.

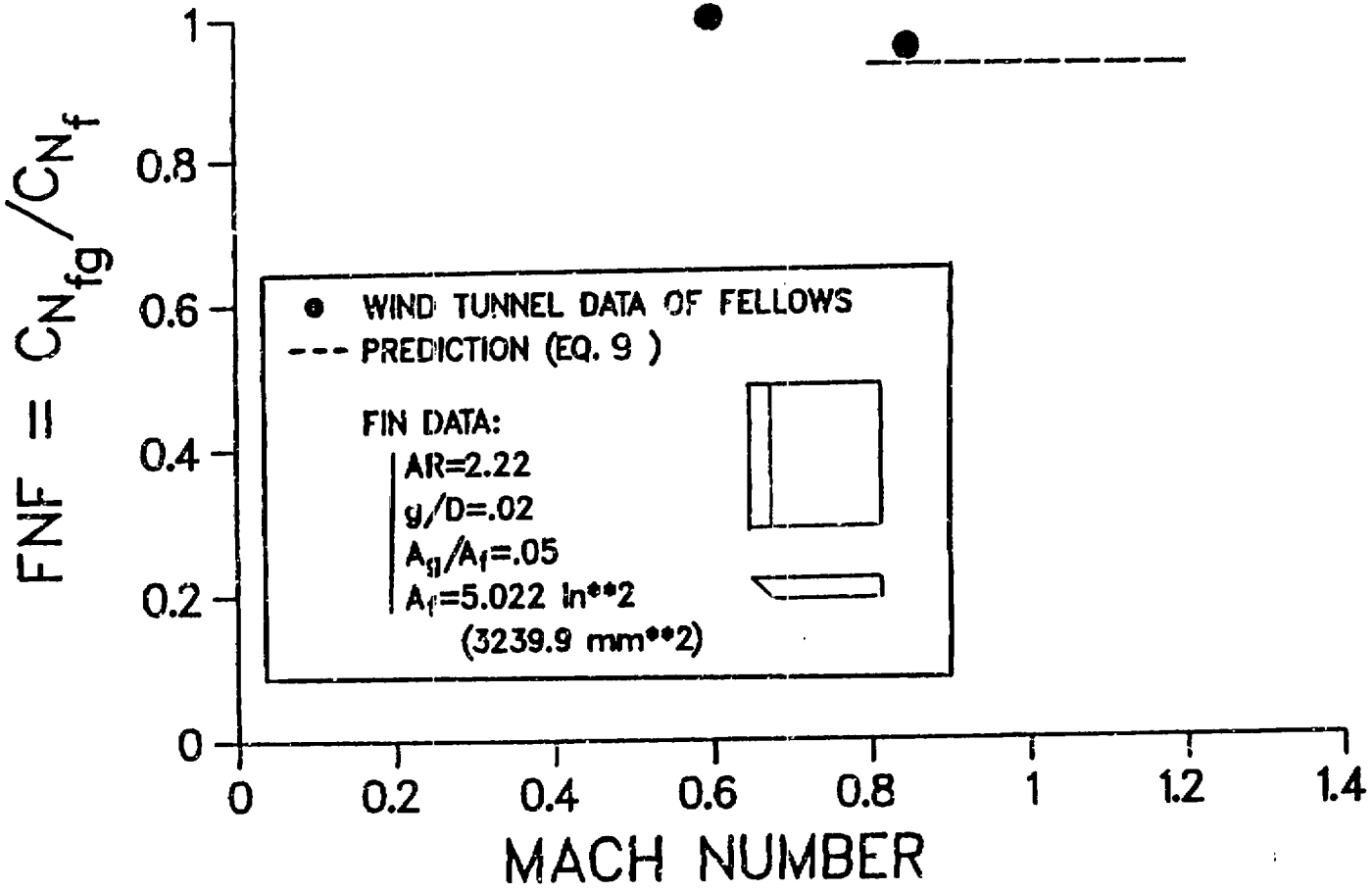

Figure 16. Comparison with data of fellows, rectangular fin of AR = 2.22.

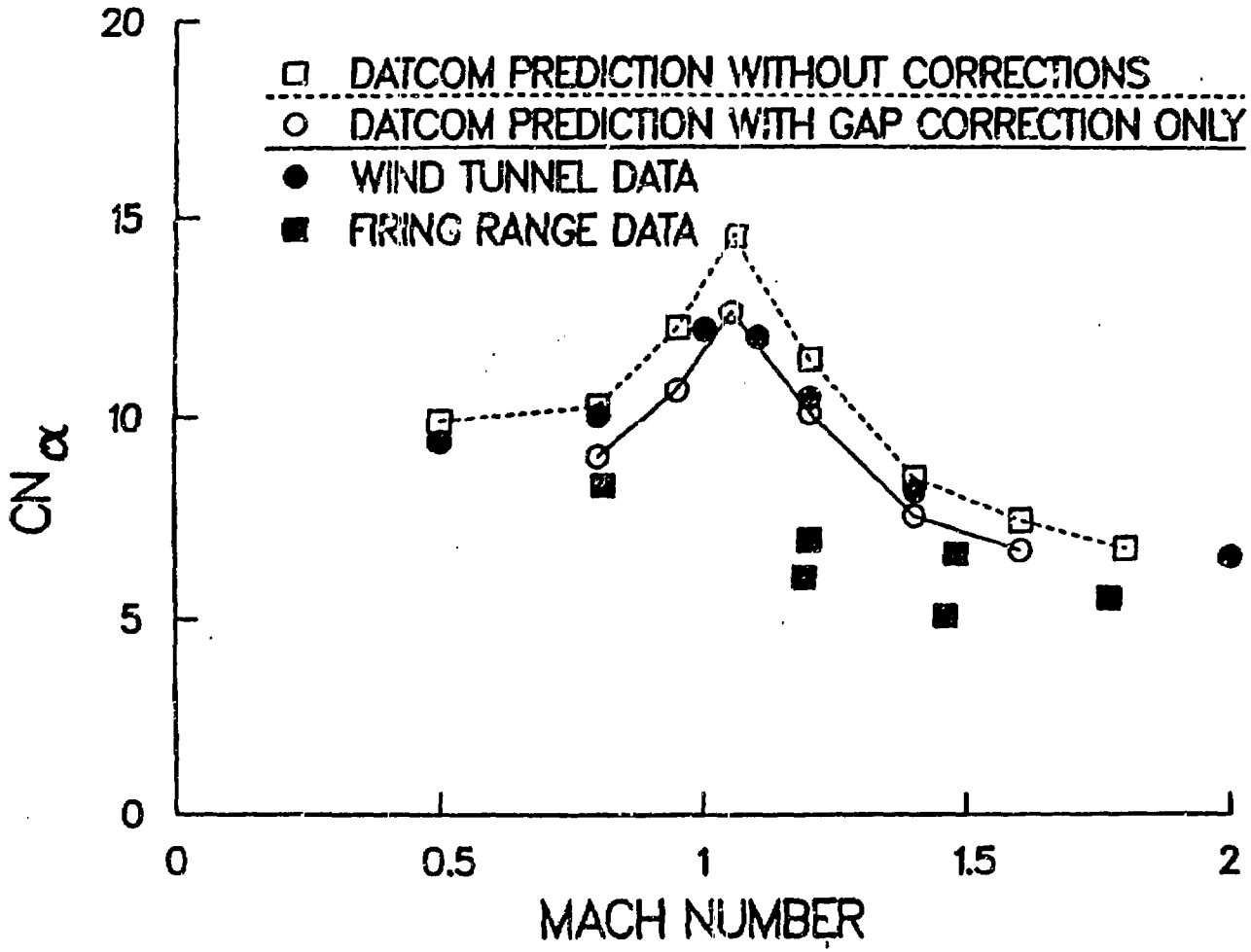

Figure 17. Gap modeling effect on the normal force slope coefficient for the Copperhead projectile.

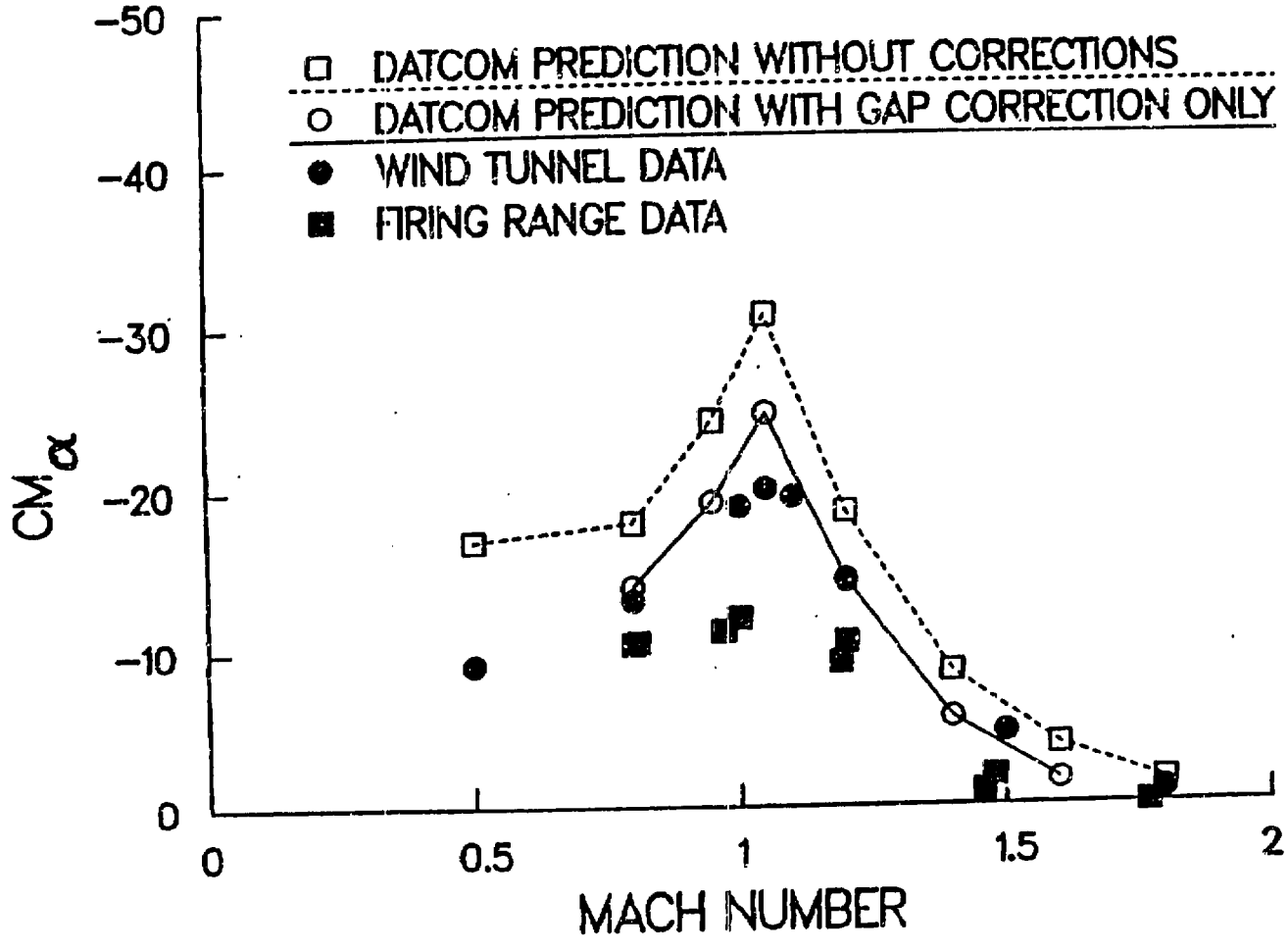

Figure 18. Gap modeling effect on the pitching moment slope coefficient for the Copperhead projectile.

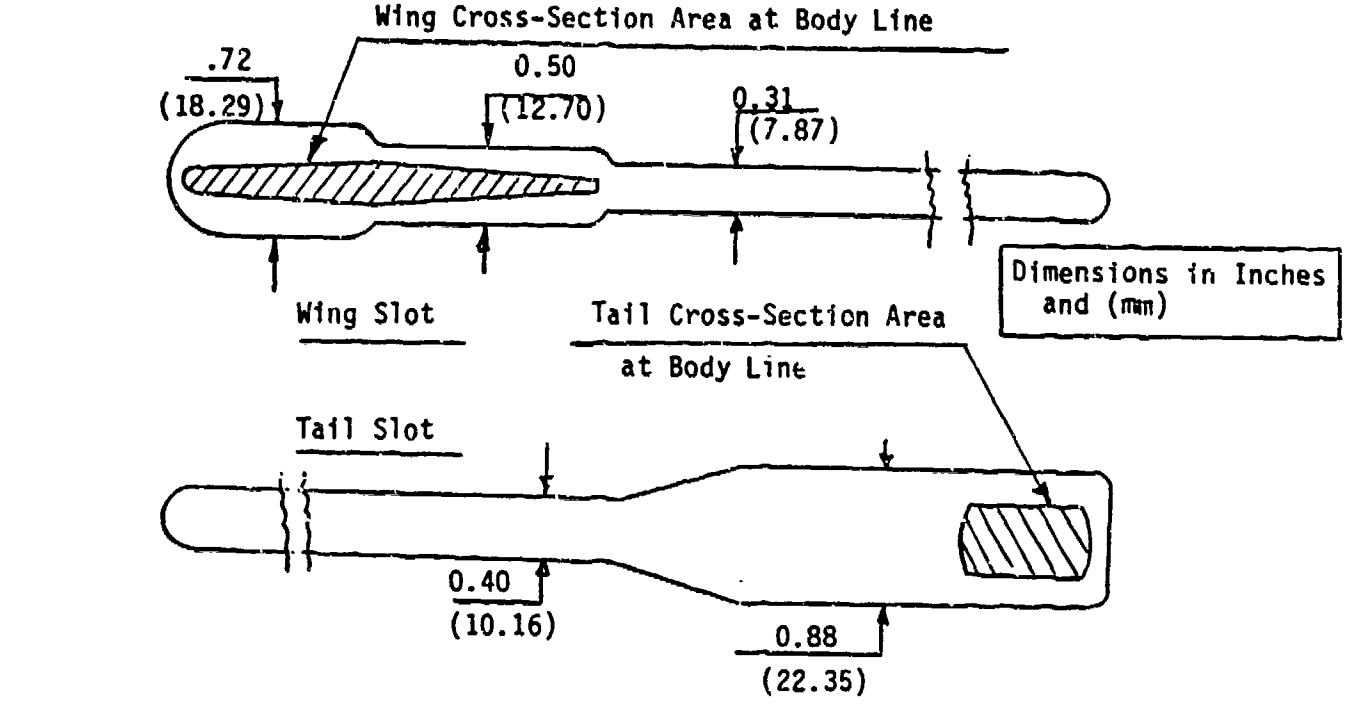

a) Wing and Tail Slot Configurations

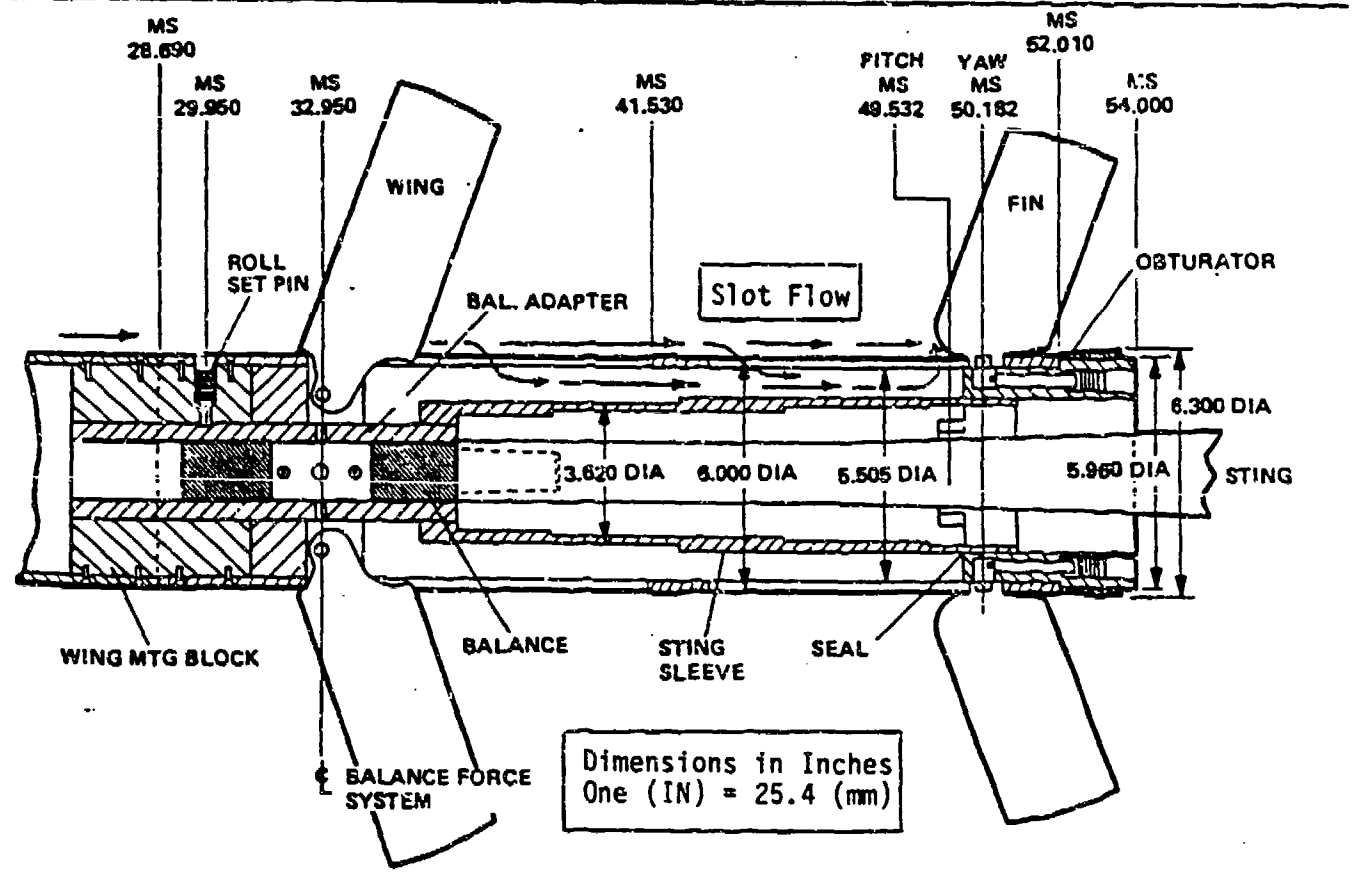

b) Wind Tunnel Model (REF) With Schematic of the Slot Flow

Figure 19. Slot configurations for the Copperhead projectile (from Reference 12).

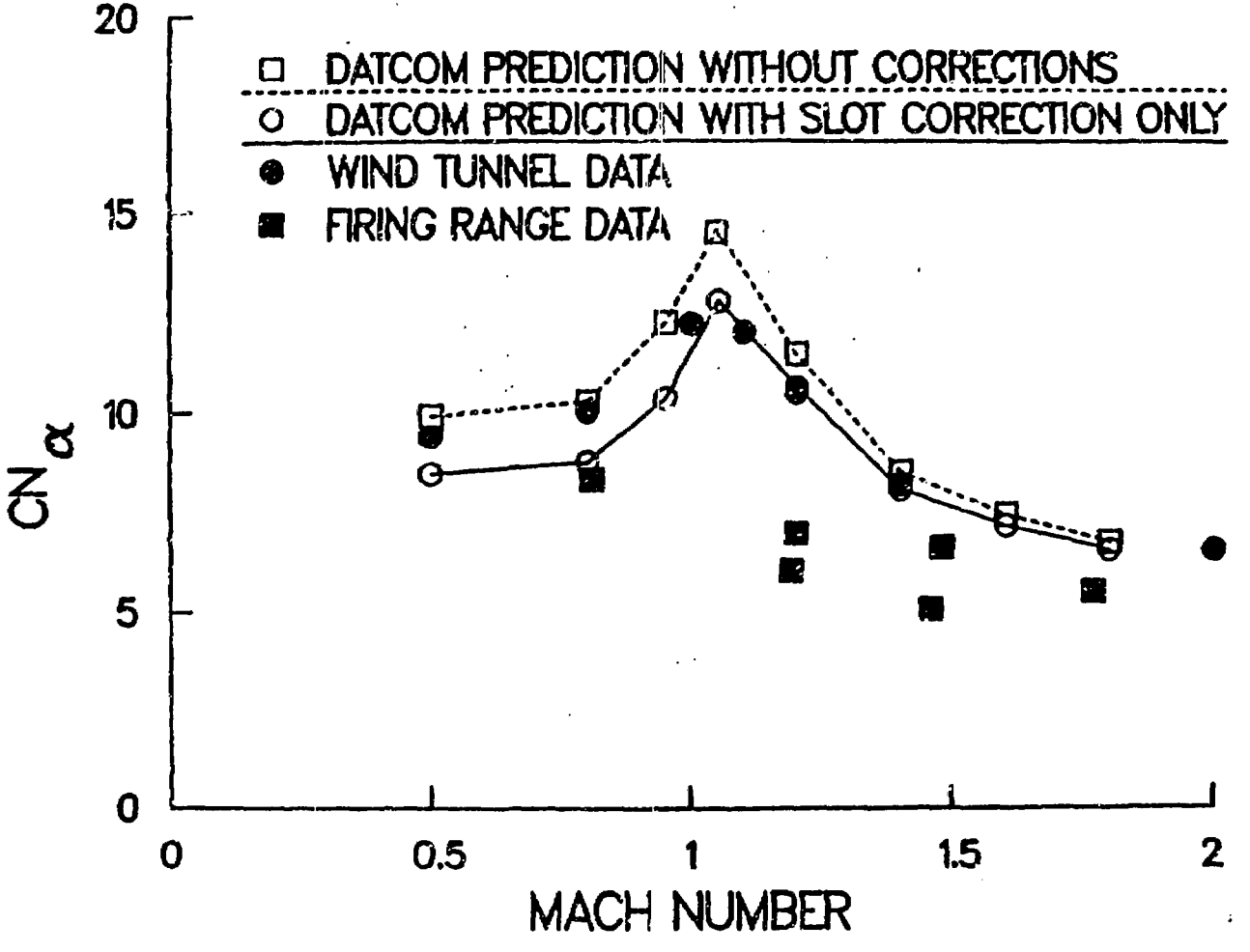

Figure 20. Slot modeling effect on the normal force slpe coefficient for the Copperhead projectile.

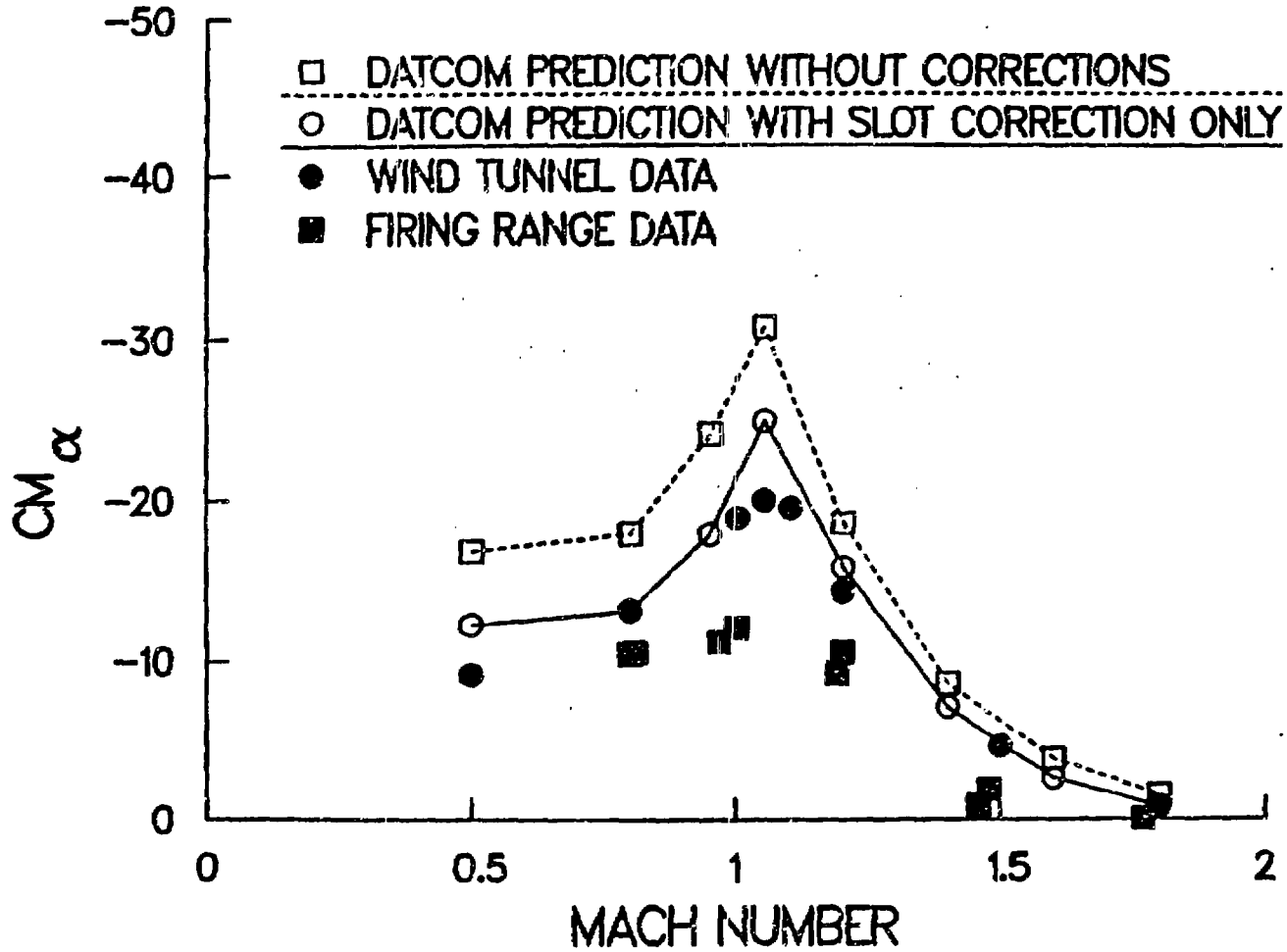

Figure 21. *Slot modeling effect on the pitching moment slope coefficient for the Copperhead projectile.*

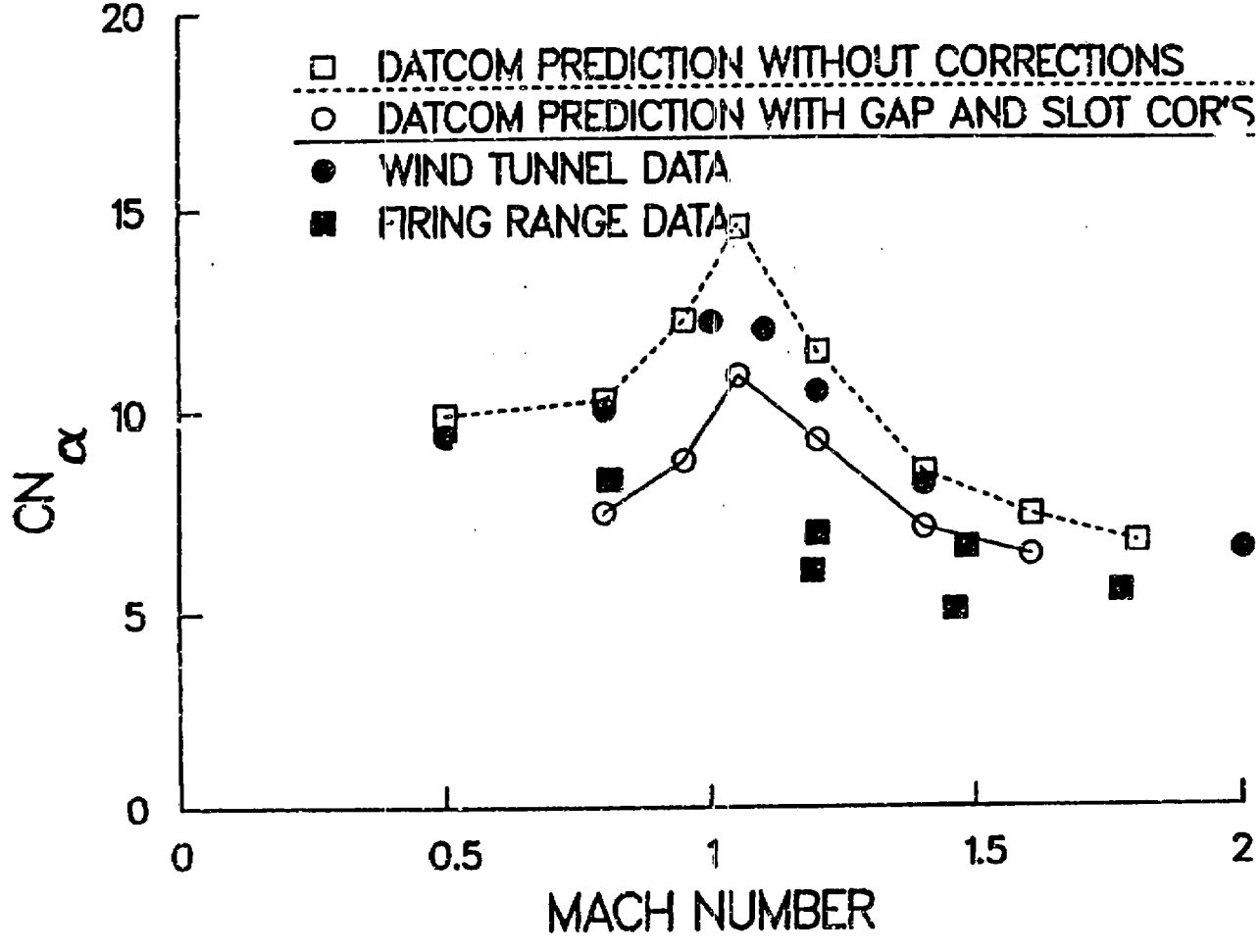

Figure 22. Gap and slot modeling effects on the normal force slope coefficient for the Copperhead projectile.

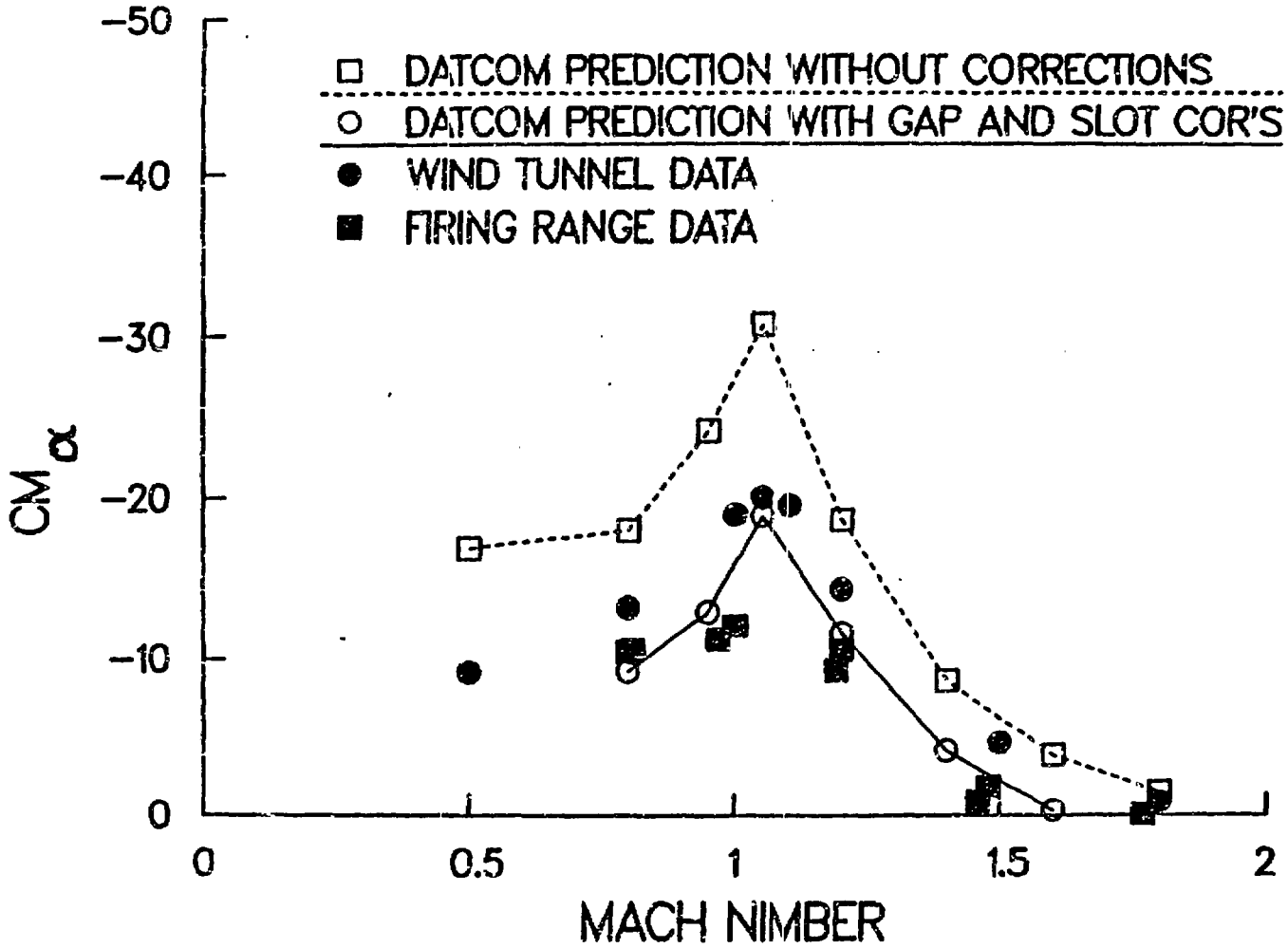

Figure 23. Gap and slot modeling effects on the pitching moment slope coefficient for the Copperhead projectile.

REFERENCES

1. Mikhail, A.G., "Application and Assessment of Two Fast Codes for a Class of Guided Projectiles," AIAA Paper No. 85-4085, October 1985. Also to appear in the Journal of Spacecraft and Rockets in the January-February issue of 1987.

2. Bleviss K.C. and Struble, R.A., "Some Effects of Streamwise Gaps on the Aerodynamic Characteristics of Low Aspect Ratio Lifting Surface at Supersonic Speeds," Douglas Aircraft Company Report SM-14627, April 1953.

3. Mirles, H. "Gap Effect on Slender Wing-Body Interference," Journal of the Aeronautical Sciences, Vol. 20, No. 8, August 1953, pp. 574-575.

4. Dugan, W.D. and Hikido, K., "Theoretical Investigation of the Effects Upon Lift of a Gap Between Wing and Body of a Slender Wing-Body Combination," NACA Technical Note No. 3224, August 1954.

5. Hoerner, S.F. and Borst, H.V., "Fluid Dynamic Lift," Book published by the authors, 1975, Chapter 20, p. 17.

6. Killough, T.L., "Investigation of Fin Gap Effects on Static Stability Characteristics of Fin Stabilized Missile," US Army Missile Command Report No. RF-TR-64-6, April 1964.

7. Dahlke, C.W. and Pettis, W., "Normal Force Effectiveness of Several fin Planforms with Streamwise Gaps at Mach Numbers of 0.8 to 5.0," US Army Missile Command Report No. RD-TR-70-8, April 1970.

8. Henderson, J.H., "An Investigation of Streamwise Body-Fin Gaps as a Means of Alleviating the Adverse Plume Effects on Missile Longitudinal Stability," US Army Missile Command Report No. RD-77-13, January 1977.

9. Fellows, K.A., "The Effects of Gap Size on the Lift and Drag of a Simple Body with Small Rectangular Wing at Subsonic Speeds," Aircraft Research Association, Lt, Test Code M49/15 Bedford, England, June 1982.

10. August H. "Improved Control Su e Effectiveness for Missiles," AIAA Paper No. 82-0318, January 1982.

11. Sun, J., Hansen, S.G., Cummings, R.M. and August, H., "Missile Aerodynamic Prediction (MAP) Code," AIAA Paper No. 84-0389, January 1984. Also Journal of Spacecraft and Rockets, Vol. 22, No. 6, November-December 1985, pp.605-613.

12. Appich, W.H., Jr. and Wittmeyer, R.E., "Aerodynamic Effects of Body Slots on a Guided Projectile," Journal of Spacecraft and Rockets, Vol. 17, No. 6, November - December 1980, pp. 522-528. Also as AIAA Paper No. 79-1658, August 1979.

13. Washington, W.D., Wittmeyer, R.E. and Appich, W.H., Jr., "Body Slot Effects on Wing-Body and Wing-Tail Interference of a Typical Cannon-Launched Guided Projectile," AIAA Paper No. 80-0260, January 1980.

REFERENCES (Continued)

14. Washington, W.D., Wittmeyer, R.E. and Appich, W.H., Jr., "Design Approach for Estimating Body Slot Effects on Wing-Body-Tail Lift," Journal of Spacecraft and Rockets, Vol. 18, No. 6, November-December 1981, pp. 481-482.

15. Appich, W.H., Jr., McCoy, R.L. and Washington, W.D. "Wind Tunnel and Flight Test Drag Comparison for a Guided Projectile with Cruciform Tails," AIAA Paper No. 80-0426, January 1980.

16. Pitts, W.C., Nielsen, J.N. and Kattari, G.E., "Lift and Center of Pressure of Wing-Body-Tail Combinations at Subsonic, Transonic and Supersonic Speeds," NACA Report No. 1307, 1959.

17. Schlichting, H., "Boundary-Layer Theory," McGraw-Hill Book Company, 6th Edition, 1968, p. 599.

LIST OF SYMBOLS

A, A_1, A_2	=	fin total surface area (one side only)
$A_{10}, A_{11}, A_{20}, A_{22}$	=	fin partial surface area (one side only)
AR	=	fin aspect ratio, $(2b)^2/S$
A_f	=	fin surface area (one side only of one fin panel)
A_g	=	streamwise gap area for one fin panel
AF	=	fin area correlation factor
b	=	fin semi span (without a gap)
b_1, b_2	=	a prescribed fin height (without a gap)
BF	=	boundary layer correlation factor
c, c_1, c_2	=	fin root chord length
CF	=	overall fin correlation factor
C_N	=	normal force coefficient (based on the body reference area) = normal force/qs_{ref}
C_{N_f}	=	fin (and its interference) normal force coefficient based on the body reference area
$C_{N_{fg}}$	=	fin (and its interference) normal force coefficient in presence of a fin gap "g"
C_{N_α}	=	normal force slope coefficient (per radian), $\partial C_N/\partial\alpha$
$C_{N_{\alpha f}}$	=	fin (and its interference) normal force slope coefficient (per radian)
$C_{N_{\alpha fg}}$	=	fin (and its interference) normal forces slope coefficient, in presence of a fin gap "g" (per radian)
C_M	=	pitching moment coefficient about the C.G. of the configuration, (pitching moment)/qs_{ref} D
C_{M_α}	=	pitching moment slope coefficient (per radian), $\partial C_M/\partial\alpha$
$C_{M_{\alpha g}}$	=	pitching moment shape coefficient (per radian) in the presence of a fin gap "g"
CSF	=	fin chord and span correlation factor
D	=	body diameter

FNF	=	fin normal force loss factor, due to presence of a fin gap "g"
g, g_1, g_2	=	gap height between fin root chord and body surface
GF	=	fin gap correlation factor
M	=	Mach number of projectile
q	=	dynamic pressure of the flow ($0.5\ \rho_\infty U_\infty^2$)
R_e, R_{e1}, R_{e2}	=	Reynolds number per unit length, $\rho_\infty U_\infty/\mu_\infty$
R_{e_x}	=	Local Reynolds number of the projectile flow, $\rho_\infty U_\infty X/\mu_\infty$
S	=	fin surface area (one side) of two fin panels connected without gaps
S_{ref}	=	body reference area, $\pi D^2/4$
SF	=	fin shape correlation factor
x	=	distance, along the body axis, from the nose tip
x_{LE}, x_{LE1}, x_{LE2}	=	distance, along the body axis, from the nose tip to the leading edge of a fin panel, at the fin root section

Greek Symbols

α	=	angle of attack
α_t	=	total angle of attack $\approx \sqrt{\alpha^2 + \beta^2}$ (for small α and β)
β	=	side slip angle
δ	=	boundary layer thickness
$\delta_{LE}, \delta_{LE1}, \delta_{LE2}$	=	boundary layer thickness at the leading edge of the fin root section

Subscript

g	=	indicates the presence of a gap between fin root chord and body surface
s	=	indicates the presence of open slot(s) on the projectile body near the fin panel

DISTRIBUTION LIST

No. of Copies	Organization
12	Administrator Defense Technical Info Center ATTN: DTIC-FDAC Cameron Station, Bldg 5 Alexandria, VA 22304-6145
1	HQDA DAMA-ART-M Washington, DC 20310
1	Commander US Army Materiel Command ATTN: AMCDRA-ST 5001 Eisenhower Avenue Alexandria, VA 22333-0001
9	Commander Armament RD&E Center US Army AMCCOM ATTN: SMCAR-MSI SMCAR-LCA-F/Hertz Friedman Loeb Kline Kahn Friedman Hudgins Grau Dover, NJ 07801-5001
1	Commander US Army Armament, Research, Development & Engineering Ctr ATTN: SMCAR-TDC Dover, NJ 07801
1	Commander US Army Jefferson Proving Ground Materiel Testing Directorate ATTN: Arthur B. Alphin, MAJ, ARM Madison, IN 47250-5100
1	Director US AMCCOM ARADEC CCAC Benet Weapons Laboratory ATTN: SMCAR-CCB-TL Watervliet, NY 12189-4050
1	Commander US Army Armament, Munitions & Chemical Command ATTN: SMCAR-IMP-L Rock Island, IL 61299-7300
1	Commander US Army Aviation Systems Cmd ATTN: AMSAV-E 4300 Goodfellow Blvd St. Louis, MO 63120-1798
1	Director US Army Aviation Research & Technology Activity Ames Research Center Moffett Field, CA 94035-1099
1	Commander CECOM R&D Technical Library ATTN: AMSEL-IM-L Fort Monmouth, NJ 07703-5000
3	Commander US Army Missile Command ATTN: AMSMI-RX Redstone Arsenal, AL 35898-5249
1	Director US Army Missile & Space Intelligence Center ATTN: AIAMS-YDL Redstone Arsenal, AL 35898
1	Commander US Army Tank Automotive Command ATTN: AMSTA-TSL Warren, MI 48397-5000
1	Director US Army TRADOC Analysis Center ATTN: ATOR-TSL White Sands Missile Range, NM 88002-5502
1	Commander US Naval Air Systems Command ATTN: AIR-604 Washington, DC 20360

DISTRIBUTION LIST

No. of Copies	Organization
1	Commander US Army Research Office P. O. Box 12211 Research Triangle Park, NC 27709-2211
1	Commander David W. Taylor Naval Ship Research & Development Ctr ATTN: Mr. Stanley Gottlieb Bethesda, MD 20084
1	Commander US Naval Surface Weapons Center ATTN: Dr. F. Moore Dr. T. Clare, Code DK20 Dahlgren, VA 22448
2	Commander US Naval Surface Weapons Center ATTN: Dr. U. Jettmar Dr. A. Wardlaw Silver Spring, MD 20910
1	Commander US Naval Weapons Center ATTN: Code 3431, Tech Lib China Lake, CA 93555
1	Commander US Army Development & Employment Agency ATTN: MODE-ORO Ft. Lewis, WA 98433-5000
1	Director NASA Langley Research Center ATTN: NS-185, Tech Lib Langley Station Hampton, VA 23365
2	Commandant US Army Infantry School ATTN: ATSH-CD-CS-OR Ft. Benning, GA 31905-5400
1	AFWL/SUL Kirtland AFB, NM 87117
1	AFATL/DOIL (Tech Info Ctr) Eglin AFB, FL 32542-5438
3	Sandia Laboratories ATTN: Dr. W.L. Oberkampf Dr. F. Blottner Division 1636 Sandia National Laboratories Albuquerque, NM 87185
3	Director NASA Ames Research Center ATTN: MS-227-8, L. Schiff Moffett Field, CA 94035
1	Massachusetts Institute of Technology ATTN: Tech Library 77 Massachusetts Avenue Cambridge, MA 02139
1	Virginia Polytechnic Institute & State University ATTN: Dr. Clark H. Lewis Department of Aerospace & Ocean Engineering Blacksburg, VA 24061
1	University of Delaware Mechanical and Aerospace Engineering Department ATTN: K.L. Palko Newark, DE 19711
10	CIA OIR/DB/Standard GE47 HQS Washington, DC 20505
1	Southwest Research Institute ATTN: Mr. T. Jeter Engineering Resources P.O. Box 28510 San Antonio, TX 78284
1	Batelle Northwest ATTN: Mr. M. Garnich P.O. Box 999 Richland, WA 99358

DISTRIBUTION LIST

Aberdeen Proving Ground

Dir, USAMSAA
ATTN: AMXSY-D
AMXSY-MP, H. Cohen

Cdr, USATECOM
ATTN: AMSTE-SI-F

Cdr, CRDEC, AMCCOM,
ATTN: SMCCR-RSP-A
SMCCR-MU
SMCCR-SPS-IL

USER EVALUATION SHEET/CHANGE OF ADDRESS

This Laboratory undertakes a continuing effort to improve the quality of the reports it publishes. Your comments/answers to the items/questions below will aid us in our efforts.

1. BRL Report Number_____ Date of Report_____

2. Date Report Received_____

3. Does this report satisfy a need? (Comment on purpose, related project, or other area of interest for which the report will be used.)_____

4. How specifically, is the report being used? (Information source, design data, procedure, source of ideas, etc.)_____

5. Has the information in this report led to any quantitative savings as far as man-hours or dollars saved, operating costs avoided or efficiencies achieved, etc? If so, please elaborate._____

6. General Comments. What do you think should be changed to improve future reports? (Indicate changes to organization, technical content, format, etc.)

CURRENT ADDRESS

Name

Organization

Address

City, State, Zip

7. If indicating a Change of Address or Address Correction, please provide the New or Correct Address in Block 6 above and the Old or Incorrect address below.

OLD ADDRESS

Name

Organization

Address

City, State, Zip

(Remove this sheet, fold as indicated, staple or tape closed, and mail.)

FOLD HERE

Director
US Army Ballistic Research Laboratory
ATTN: DRXBR-OD-ST
Aberdeen Proving Ground, MD 21005-5066

NO POSTAGE
NECESSARY
IF MAILED
IN THE
UNITED STATES

OFFICIAL BUSINESS
PENALTY FOR PRIVATE USE, $300

BUSINESS REPLY MAIL
FIRST CLASS PERMIT NO 12062 WASHINGTON, DC
POSTAGE WILL BE PAID BY DEPARTMENT OF THE ARMY

Director
US Army Ballistic Research Laboratory
ATTN: DRXBR-OD-ST
Aberdeen Proving Ground, MD 21005-9989

FOLD HERE